

## **Piezoelectric Materials Used in Underwater Acoustic Transducers**

Huidong Li, Z. Daniel Deng\* and Thomas J. Carlson

Energy and Environment Directorate, Pacific Northwest National Laboratory, P.O. Box 999,

Richland, Washington 99352, USA

Huidong Li

Tel.: 1-509-371-6185; Fax: 1-509-372-6089; e-mail: [huidong.li@pnnl.gov](mailto:huidong.li@pnnl.gov)

Z. Daniel Deng

Tel: 1-509-372-6120; Fax: 1-509-372-6089; e-mail: [zhiqun.deng@pnnl.gov](mailto:zhiqun.deng@pnnl.gov)

Thomas J. Carlson

Tel.: 1-503-417-7562; Fax: 1-503-417-2175; e-mail: [thomas.carlson@pnnl.gov](mailto:thomas.carlson@pnnl.gov)

\* Corresponding author

**Abstract:** Piezoelectric materials have been used in underwater acoustic transducers for nearly a century. In this paper, we review four different types of materials—piezoelectric ceramics, single crystals, composites, and polymers—which are currently widely used in underwater acoustic transducers. Piezoelectric ceramics, the most dominant material type, are used as single-phase materials or as one of the end members in composites. Piezoelectric single crystals offer outstanding electromechanical response but are limited in use by their manufacturing cost. Piezoelectric polymers provide excellent acoustic impedance matching and transducer fabrication flexibility, but their piezoelectric properties are not as good as those of ceramics and single crystals. Composites combine the merits of ceramics and polymers and are receiving increased attention. The typical structure and electromechanical properties of each of the four material types are introduced and discussed with respect to underwater acoustic transducer applications. Their advantages and disadvantages are summarized. Some of the critical design considerations when developing underwater acoustic transducers with these materials are also discussed.

**Keywords:** Underwater Acoustic Transducers; Hydrophones; Transmitters; Piezoelectricity; PZT Ceramics; Single Crystals; Composites; Polymers; Acoustic Telemetry.

## **1. INTRODUCTION**

An acoustic transducer converts mechanical energy of sound waves into electric energy (hydrophones, microphones) or converts electric energy into sound waves (transmitters, loudspeakers). For underwater acoustic transducers, piezoelectric materials with lead zirconate titanate (PZT) ceramics are the dominant active materials because of their low electrical losses and high coupling coefficients.<sup>1</sup> Piezoelectricity is the ability of some materials to generate an electrical charge in response to a mechanical stress and vice versa.

This article reviews four different types of piezoelectric materials—piezoelectric ceramics, single crystals, composites and polymers—used in today’s underwater acoustic transducers (hydrophones and transmitters). The properties of these materials relevant to underwater transducers are introduced, and the ways in which these properties relate to the transducer performance are explained. The advantages and disadvantages with respect to underwater acoustic applications of each material type are summarized. Some of the critical design considerations when developing underwater acoustic transducers with these materials also are discussed.

## **2. BACKGROUND**

### **2.1 History Overview**

Piezoelectricity was first discovered by J. and P. Curie in single crystals in 1880. However, it was not utilized in underwater acoustic applications until 1917, when French physicist Paul Langevin used quartz, a piezoelectric crystal, in his hydrophone as part of a research effort to

develop underwater acoustic transducers for detecting submarines. Later, a quartz transducer was also employed in his sound projector. Further improvements in the transducer designs led to the first successful detection of a submarine in early 1918. After World War I, synthetic Rochelle salt crystal with higher piezoelectricity than quartz was used to build electroacoustic transducers with improved performance, which opened up the era of man-made piezoelectric materials for underwater acoustic transducers. World War II and the following Cold War greatly promoted research for better transduction materials to further improve the acoustic transducer performance. Ammonium dihydrogen phosphate (ADP) and lithium sulfate crystals were discovered. Then in 1944, strong piezoelectricity was found in permanently polarized barium titanate ( $\text{BaTiO}_3$ ) ceramics. Ten years later, PZT was discovered to have even better piezoelectric properties.<sup>2</sup> Following this discovery, a number of doping studies of PZT yielded an entire family of PZT polycrystalline ceramics (PZT ceramics hereinafter) that possess a wide range of dielectric and piezoelectric properties for various transducer applications. These developments accelerated the adoption of piezoelectric materials, especially piezoelectric ceramics for use in underwater acoustic transducers for naval and many other applications, because of their excellent electromechanical properties and low fabrication cost.

Due to the attractive properties of PZT ceramics, PZT single crystals, which have ordered crystalline structure throughout the entire material (hence higher piezoelectric properties after being polarized), were considered by many to be the next generation of piezoelectric materials to be widely utilized by the transducer industry. However, no PZT crystals of usable sizes could be grown successfully,<sup>3,4</sup> which maintained the dominance of PZT ceramics in the piezoelectric-based industry until now. Lead-based piezoelectric single crystals started to receive attention relatively recently in 1982 when Kuwata et al. reported an extremely high piezoelectric coupling

factor ( $> 0.9$ ) in single crystals of the solid solution of lead zinc niobate (PZN) and lead titanate (PT).<sup>5</sup> The first ultrasonic transducer patent based on PZN-PT single crystals was issued to Toshiba in 1994.<sup>6</sup> Another important piezoelectric single crystal for use in the transducer industry, the solid solution of another relaxor material, lead magnesium niobate (PMN), and PT was reported by Park and Shrout at Pennsylvania State University in 1990.<sup>7, 8</sup> They published a comprehensive report of the dielectric and piezoelectric properties of the PZN-PT and PMN-PT single crystals of several compositions and various crystallographic cuts.<sup>9</sup> It was shown that the piezoelectric constant ( $d_{33}$ ) of these single crystals could be a few times higher than those of PZT ceramics and their longitudinal coupling factor could be as high as 0.92, whereas the coupling factors for PZT ceramics were no higher than 0.77. Because of the higher sensitivity and bandwidth that lead-based single crystals provide over traditional PZT ceramics in underwater acoustic transducers, they have become the focus of a great deal of research.

These structurally and compositionally homogeneous ceramics and single crystals can also be combined with a passive polymer material to form composites. Such composites increase material flexibility and improve acoustic matching between the active material and the medium in which the acoustic wave travels. Frequently these properties cannot be achieved in single-phase ceramics and single crystals. Newnham et al. first introduced the use of piezoelectric composites in transducers.<sup>10, 11</sup> This material type quickly received attention from the acoustic transducer designers and manufacturers, especially for low-frequency underwater hydrophone applications, in which some piezoelectric composites demonstrated sensitivities that were a couple of orders of magnitude higher than traditional PZT ceramics.

The fourth type of piezoelectric material used in underwater acoustic transducers is piezoelectric polymers. These materials have much weaker piezoelectricity, high dielectric loss,

very low dielectric constants, and difficulty with electrode adhesion, compared with the other three types of piezoelectric materials. However, they have the advantages of better acoustic matching with water, increased manufacturing flexibility and extremely broad bandwidth. Their flexible nature allows them to be easily fabricated into sheets with large areas; they can also be dissolved and coated onto various surfaces. The representatives of this family are polyvinylidene difluoride (PVDF) and the co-polymers based on PVDF, such as poly(vinylidene fluoride-trifluoride) [P(VDF-TrFE)], poly(vinylidene fluoride-tetrafluoroethylene) [P(VDF-TeFE)], and poly(vinylidene cyanide-vinylacetate) [P(VDCN-VAC)]. PVDF was patented by Ford and Hanford and assigned to E. I. du Pont de Nemours and Company in 1948 before the discovery of PZT ceramics.<sup>12</sup> However, its piezoelectricity was not discovered until 1969 by Kawai.<sup>13</sup> He found that PVDF turns into a polarizable phase showing a considerable amount of piezoelectricity when stretched approximately four to five times its original lateral dimensions. Piezoelectric polymers are often used in hydrophones<sup>14-16</sup> because of their much higher hydrostatic piezoelectric voltage constant and excellent acoustic impedance matching with water. These properties are essential for hydrophone applications where higher efficiency of conversion of mechanical energy of the sound wave in water impinging on the piezoelectric material into electrical signals is highly beneficial to optimize the performance of transducers.

## **2.2 Piezoelectricity**

Piezoelectricity results from the displacement of the center of the positive charges from that of the negative charges in a piezoelectric material. This displacement can be caused either by lowering the temperature below a critical point called Curie point  $T_c$  (ceramics and single crystals) or by mechanically deforming the material (polymers).

The typical structure of piezoelectric ceramics and single crystals is the perovskite structure with a general formula of  $ABO_3$  in which A and B are cations. All of the most important piezoelectric ceramics and single crystals used in acoustic transducer applications today, such as PZT, PZN-PT, PMN-PT and  $BaTiO_3$ , belong to this category. Figure 1 illustrates the perovskite structure using  $BaTiO_3$  as an example. When the temperature is above the Curie point of the material, the structure can be described as a cubic cell. The smaller cation (B, titanium in this case) is in the body center, the larger cation (A, barium in this case) is on the corners, and the oxygens (O) are in the centers of all six faces. When the temperature is lowered below the Curie point, the titanium ion moves away from the center of the cell along one of the two orthogonal axes connecting the titanium and the oxygens, elongating the cell in the corresponding direction and resulting in a spontaneous polarization. When an electric field larger than a critical value (called the coercive field or  $E_c$ ) is applied, this spontaneous polarization is reversible and can be switched to any crystallographic axis allowed by the structure. The reversibility of a polar crystal by means of an applied electric field is called ferroelectricity.<sup>17</sup> Therefore, PZT, PZN-PT, PMN-PT, and  $BaTiO_3$  all are ferroelectrics. These materials can be synthesized into either ceramics or single crystals. The difference between a single crystal and a ceramic of the same material is that a single crystal has continuous crystal lattice (i.e., the repetition of the cell illustrated in Figure 1) throughout the entire sample, whereas the ceramic is an agglomeration of small crystals (ceramic grains) “fused” together in a random manner. Within a ferroelectric single crystal or a single grain of a ceramic, there are small regions of dipoles with uniform orientations called domains. For an as-fired ferroelectric ceramic or an as-grown single crystal, the polarization of the individual domains and grains cancel each other; the material thus is not piezoelectric. A “poling” step, in which a sufficiently high electric field is applied to the material (usually at an

elevated temperature lower than the Curie point) to switch the dipoles toward the direction of the applied field, is necessary to induce piezoelectricity.

The piezoelectricity of most of the important piezoelectric polymers, such as nylon, PVDF, and its co-polymers, also arises from ferroelectricity. These polymers are usually semi-crystalline with crystalline regions embedded inside an amorphous matrix.<sup>18, 19</sup> They typically possess non-polarizable phases after cooling from melt during the fabrication process. To become piezoelectric, stretching or drawing these polymers uniaxially or biaxially is required to convert non-polar phases into polar ones, and a poling treatment is applied to align dipoles as in the case of ceramics and single crystals.<sup>13, 20, 21</sup> The dipolar alignment mechanism during the poling process of the polymers differs from that of ceramics/single crystals in that the dipole reorientation is achieved by polymer chain rotation about the C–C axis,<sup>22</sup> whereas ceramics and single crystals are reoriented by movement of ferroelectric domain walls.

### **3. PIEZOELECTRIC CERAMICS**

#### **3.1 PZT Ceramics**

Piezoelectric ceramics have been used extensively in underwater acoustic transducers, and PZT has been the most important family in piezoelectric ceramics because of their excellent piezoelectric properties, high Curie points and a wide range of properties that they can offer by small changes in composition.<sup>23</sup> Pure PZT is a solid solution of  $\text{PbZrO}_3$  and  $\text{PbTiO}_3$ . Similar to  $\text{BaTiO}_3$ , it has the  $\text{ABO}_3$  perovskite structure shown in Figure 1; however, the B sites in the crystalline lattice of PZT are shared by  $\text{Zr}^{4+}$  and  $\text{Ti}^{4+}$ . The phase diagram of  $\text{PbZrO}_3$ - $\text{PbTiO}_3$  in Figure 2 shows how PZT transforms from a ferroelectric tetragonal phase into a ferroelectric



rhombohedral phase when the  $\text{PbZrO}_3$  concentration in the solid solution is increased to around 53 mol%. This phase transformation is almost independent of temperature, indicated by a nearly vertical line in the phase diagram. Near this phase boundary, the two ferroelectric phases coexist (a morphotropic phase boundary, or MPB). The Curie point of PZT at this MPB reaches above 350°C. Jaffe et al.<sup>2</sup> discovered the sharp increase in the piezoelectric properties at this MPB, as shown in Figure 3, which sparked tremendous interest from the transducer industry and resulted in the replacement of  $\text{BaTiO}_3$  by PZT in most transducer applications. The abrupt increase of the piezoelectric properties of PZT at the MPB is thought to result from the combined number of crystalline axes of the two coexisting phases to which the ferroelectric dipoles of the material can switch during the poling process.<sup>17</sup> Therefore, finding or constructing an MPB in a two-component solid solution has become an important approach to enhance the piezoelectric properties of piezoelectric ceramics.

Over the past few decades, a large variety of additives or dopants have been used to compositionally modify PZT so its properties can be tailored for a wide range of transducer applications. The additives are typically subdivided into three categories based on their valences with respect to those of the elements in PZT which they are presumed to substitute for because of the similarity in atomic radii: (1) isovalent additives such as Sr, Calcium, Ba (for Pb) and Sn (for Zr or Ti); (2) donor additives such as La (for Pb), Nb (for Zr and Ti); and (3) acceptor additives such as K (for Pb) and Fe (for Zr and Ti). The effects of isovalent additives on the piezoelectric and dielectric properties of PZT are relatively small compared to those of the donor and acceptor additives. They generally result in higher permittivity and low mechanical or dielectric loss. Acceptor additives generally introduce “harder” characteristics to PZT than the isovalent additives—lower permittivity and dielectric loss, lower electromechanical coupling, and better

linearity under high-voltage driving conditions. Donor additives usually cause PZT to exhibit “soft” characteristics: higher permittivity and dielectric loss, higher electromechanical coupling, lower mechanical quality factor  $Q$ , poor linearity at high driving voltages, and easier depolarization.

According to U.S. military standard MIL-STD-1376B (SH), piezoelectric ceramics are categorized into six different types: Navy Type 1 through Navy Type 6.<sup>24</sup> Isovalent-additive-modified PZTs are classified as Navy Type 1. For medium- or high-drive sonar applications, heat generation is a primary concern because the transducer usually operates at its resonance. Heat generation becomes an important concern for the longevity of the transducer. Therefore, Navy Type 1 piezoelectric ceramics are preferred for these applications because of their high mechanical  $Q$  and low dielectric loss. For applications in which stability under high electric drive is most critical and where compromise of electromechanical performance is acceptable, acceptor-modified PZT ceramics (Navy Type 3) are the materials of choice. Because donor-modified PZTs have higher charge sensitivity at the expense of higher mechanical and dielectric loss, they are classified as Type 2 materials, suitable for passive transducer applications such as hydrophones but not for active acoustic radiating applications. Navy Type 4 piezoelectric ceramics are modified  $\text{BaTiO}_3$  compositions with lower piezoelectric activity and a lower Curie temperature than any of the PZT ceramics. They are usually not used in transducers.<sup>25</sup> Navy Type 6 ceramics are similar to those of Navy Type 2 but with enhanced piezoelectric activity, higher dielectric constant, and lower Curie temperatures. Type 5 is an intermediate type between Navy Type 2 and Navy Type 6. Table 1 lists some of the typical properties of these piezoelectric ceramics. In addition to these Navy types, other custom formulations of PZT are commercially available for special transducer applications.

The effects of differences in the piezoelectric performance of different types of PZT ceramics are put into perspective in Figure 4 which shows differences in the source level of a miniaturized underwater fish tag transmitter that uses a hollow cylindrical PZT transducer.<sup>26-28</sup>

It is worth noting that the piezoelectric properties of PZT ceramics can be changed by an applied direct current (DC) bias field or by stress. In underwater sound projectors, a PZT ceramic can be implemented using a DC bias to achieve higher acoustic power without risk of depolarization. Moffett et al.<sup>29</sup> demonstrated that the source level of a PZT sound projector could be enhanced by more than 10 dB by using a DC bias field of 12 kV/cm. For sonar projectors, especially those used in submarines, the PZT ceramics experience hydrostatic stress, with magnitude dependent on the depth of the submarine. In many cases, the PZT is also subject to a compressive bias stress (or “pre-stress”) in order to alleviate the more detrimental tensile stress during operation. When the stress level is not too high (<40 MPa), the  $d_{33}$  of PZT increases with increasing stress because of the stress-driven movement of non-180° domain walls. The  $d_{33}$  of soft PZT shows much greater enhancement with stress than that of hard PZT.<sup>30, 31</sup> However, when the stress level is too high, depolarization starts to occur, resulting in decreased  $d_{33}$ .

### **3.2 Relaxor Ferroelectric Ceramics**

Another important group of piezoelectric ceramics used in underwater acoustic transducers is relaxor ferroelectric materials, such as PMN-based, PNN (lead nickel niobate)-based and PZN-based relaxors. Relaxor ferroelectrics have the general formula of  $\text{Pb}(\text{B}'\text{B}'')\text{O}_3$ . Due to the existence of micro regions containing short-range order of B' and B'' ions,<sup>8, 32</sup> the most typical characteristic of these materials is their dispersive phase transitions. In dispersive phase transitions, ferroelectric–paraelectric phase transitions display both temperature and frequency

dispersion. For normal ferroelectrics, the ferroelectric–paraelectric phase transitions are an abrupt change at their Curie points and their Curie points are independent of frequency. However, for relaxor ferroelectrics, their ferroelectric–paraelectric phase transitions are gradual, so their permittivity as a function of temperature shows a broad peak. Therefore,  $T_m$ , the temperature at which the permittivity is maximal, is used instead of  $T_c$  to denote the approximate phase transition point. In addition, the value of  $T_m$  is frequency dependent. It typically shifts towards a higher temperature as frequency increases.

The electromechanical response of these relaxor materials is somewhat more complex than that of PZT. At room temperature, PMN has cubic structure and thus is not piezoelectric but electrostrictive instead. Electrostriction is an effect where strain is generated under an applied electric field because of the displacements of the positive charge and the negative charge under the electric field. This effect is usually very small and occurs in all materials, regardless of their structure symmetries, while piezoelectricity requires lack of center symmetry (e.g., the B-site ion moves off the center of the cell when the temperature is below the Curie point, as demonstrated in Figure 1). The strain caused by piezoelectricity is in the same direction of the applied electric field and is directly proportional to the strength of the electric field, whereas the strain caused by electrostriction is independent of the polarity of the field and is proportional to the second power of the field strength.

PMN, PNN, and PZN by themselves are strongly electrostrictive. However, when mixed with  $\text{PbTiO}_3$  to form solid solutions, these materials become more and more piezoelectric as the concentration of PT increases. Very strong piezoelectric properties are observed in these solid solutions, especially when driven under a high electric field. In ferroelectrics such as PZT, PMN-PT, and PZN-PT, as long as the applied electric field is not too much higher than the coercive

field  $E_c$ , the induced strain is induced by both ferroelectric domain reorientation and electrostriction. The piezoelectric properties of some important PMN-PT and PNN-PT ceramics are also listed in Table 1.

For underwater acoustic transducers, a high electromechanical coupling factor  $k$  is always desired to maximize the efficiency of the transducer because the square of  $k$  represents the fraction of the input electrical energy converted into mechanical energy (in the cases of sound projectors) or vice versa (in the cases of hydrophones).

Mechanical quality factor ( $Q_m$ ) describes the sharpness of a resonant response curve. It can be estimated using the following equation<sup>1</sup>:

$$Q_m = \frac{f_r}{(f_1 - f_2)} \quad (1)$$

where  $f_r$  is the mechanical resonance frequency and  $f_2$  and  $f_1$  are the frequencies at one-half power relative to the power at resonance. The “bandwidth” is the frequency span in which an acoustic transducer can operate effectively under a given criteria. However, there is not a definition that is universally accepted.<sup>33</sup> Traditionally,  $1/Q_m$ , namely “ $(f_2 - f_1)/f_r$ ” is considered to be the bandwidth (or “fractional bandwidth”) of a transducer, covering a frequency range where the output power is within 3 dB of the value at resonance. Sometimes, a -6 dB criteria, instead of -3 dB, is also used to define the fractional bandwidth of an acoustic transducer. When characterizing the bandwidth of a piezoelectric material, a bandwidth definition of  $(f_{ar} - f_r)/f_r$  is also used, where  $f_{ar}$  is the antiresonance frequency of the piezoelectric specimen.<sup>34</sup>  $Q_m$  affects the resolution, efficiency, and bandwidth of the transducer. A small value of  $Q_m$  is usually preferred for low-drive or non-resonant applications because it indicates a broad bandwidth and that a shorter pulse (faster “ring-down”) can be obtained so a higher temporal resolution of the signal

can be achieved. A low  $Q_m$  is usually achieved by acoustic impedance matching of the transducer and the medium, providing better acoustic energy transfer between the transducer and water. For high-power or near-resonance sound projectors, however, a high  $Q_m$  is desired to minimize the energy loss of the transducer during operation.

Dielectric loss factor ( $\tan\delta$ ) is a measure of how much electrical energy is lost as heat during the operation of piezoelectric ceramics. It is always preferable to have this loss as low as possible. A low  $\tan\delta$  ensures that a transducer will not overheat during operation, especially during high voltage drive conditions and high duty cycles. The dielectric loss factors of the piezoelectric ceramics used in underwater acoustic transducers typically do not exceed 0.03.

The permittivity and elastic compliance of the material are also important when one considers a piezoelectric ceramic for a specific underwater acoustic transducer. The permittivity of the piezoelectric ceramic dictates in part the capacitance of the transducer and thus affects ability of the available power source to drive the transducer, especially for transducers that operate at mid or high ultrasonic frequencies (a few hundred kHz and above). At those frequencies, the piezoelectric transducer is usually relatively small. A small change in transducer dimensions may cause large change in the transducer capacitance. The elastic compliance of the piezoelectric ceramics directly relates to the frequency constants of the material. Thus, it affects the dimensions of the transducer given the operating frequency needed for a particular application.

### **3.4 Other Piezoelectric Ceramics**

Because of the toxicity of lead-based ferroelectric ceramics, lead-free piezoelectric ceramic materials also have been studied as the alternatives to the toxic lead-based ones.<sup>35</sup> The important

lead-free piezoelectric ceramics which have been explored include alkaline niobates such as sodium potassium niobate (KNN), bismuth sodium titanate (BNT), bismuth layer-structured ferroelectrics (BLSF), aluminum nitride (AlN) and zinc oxide (ZnO). In addition to the fact that they are much more environmentally friendly, their lower densities are also advantageous in underwater transducers due to expected better acoustic impedance matching. However, the major drawback of these materials is that at present their piezoelectric properties are all inferior to those of lead-based ferroelectrics. Also, unlike PZT ceramics having dozens of variants for a wide range of applications, lead-free piezoelectrics are only used in very specific applications, mainly the high-frequency ones.<sup>36</sup> Among the lead-free materials, KNN has shown the greatest potential because of its relatively high piezoelectric performance. The highest piezoelectric coefficient  $d_{33}$  for lead-free piezoelectrics reported to date, 416 pC/N, was achieved by both compositionally and structurally modifying this material.<sup>37</sup>

Unlike lead-based ferroelectrics, KNN and BNT, which all have perovskite structure, both AlN and ZnO have wurtzite structure and do not possess ferroelectricity. Their piezoelectricity arises from the lack of center symmetry in the unit cells. Therefore, in comparison with perovskite ferroelectrics, they have much smaller piezoelectric response ( $d_{33}$  of AlN is 5.5 pC/N<sup>38</sup> and that of ZnO is 10-12 pC/N<sup>39</sup>), thus making them unsuitable for actuation-type applications such as sound projectors. However, their low permittivity (only 8-12<sup>40</sup>) in contrast to 800-7000 for lead-based ferroelectrics) makes them good candidates for acoustic sensing applications. It is worth noting that the piezoelectric properties of ZnO can be greatly enhanced by adding dopants to induce ferroelectricity. Most recently, Feng et al. successfully improved the  $d_{33}$  of ZnO to 170 pC/N by doping it with 2.5 mol% of Vanadium.<sup>41</sup>

These materials are typically fabricated into thin films as high frequency ultrasonic transducers because of the compatibility of their fabrication process with existing semiconductor manufacturing process.<sup>42</sup> It is important that the deposition process of these thin films result in films oriented in the polar c-axis so the c-axis can be in parallel with the applied electric field to enable piezoelectricity.<sup>40, 42</sup> The most common technique for depositing AlN and ZnO thin films is sputtering, as this method produces oriented thin films with uniform thickness on a variety of substrates.<sup>43</sup>

### **3.5 Fabrication of Piezoelectric Ceramics**

Industrial fabrication of piezoelectric ceramics used in acoustic transducers can be divided into two categories based on the target thickness of the ceramic. For piezoelectric ceramics with thickness greater than 10-20 microns such as bulk ceramics and thick films, the most common way to fabricate piezoelectric ceramics is the conventional mixed-oxide method, in which the following processing steps are involved:

- 1) Powder mixing: raw powders of individual oxides are weighed and mixed first according to the stoichiometry of the ceramic formula. In most cases, excess PbO is added to compensate the lead loss due to the evaporation of lead during the later high-temperature heat treatment steps of the ceramics.
- 2) Forming: the powder mixture is then processed to form the necessary geometric shape by a variety of forming technique, such as cold pressing, tape casting, slip casting, extrusion, screen printing, injection molding etc., according to the end application of the ceramic.



- 3) Calcination and sintering: after the forming step, the “green” ceramic body is subjected to a series of high-temperature heat treatments to burn out the organic species introduced during the mixing and forming steps, form the appropriate material phase (the calcination step), and eliminate the pores in the ceramic body and fine-tune the microstructure (the sintering step). The sintering step usually requires a temperature of 900-1250°C. At such high temperature, evaporation of PbO is significant due to the low melting point (886°C), causing lead loss in the final ceramics. Therefore, during the powder mixing step, excess PbO is typically added to compensate the lead loss, and various atmosphere control techniques are also implemented during firing.
- 4) After heat treatment, the ceramic is processed into the final shape required by specific applications, which may involve lamination, cutting, lapping, polishing, etc., followed by electroding and poling so the ceramic becomes piezoelectric.

In cases where the ceramic thickness is 20 microns or smaller, thin film deposition and microfabrication techniques are usually utilized. Piezoelectric thin films can be deposited either by physical vapor deposition (PVD) or chemical methods such as chemical solution deposition and chemical vapor deposition (CVD). PVD methods are carried out in vacuum. They use physical means such as electron beam, heat or plasma to vaporize a ceramic target (the source material) into atoms or ions to deposit thin films on substrates. Chemical methods deposit thin films by reacting different precursors on the substrate surface.

The above techniques provide a general picture of the fabrication processes of piezoelectric ceramics. Detailed discussions of these techniques are beyond the scope of this review. One can consult extensive literature on these topics.

#### 4. PIEZOELECTRIC SINGLE CRYSTALS

Piezoelectricity was known to be present in piezoelectric single crystals long before it was found in piezoelectric ceramics.<sup>17</sup> Quartz, a single crystal of  $\text{SiO}_2$ , was the first piezoelectric material used in underwater acoustic transducers.<sup>1</sup> In recent decades, it has also been micromachined into thin film geometry to be used as microbalances to conduct sensitive measurements of small substances in water.<sup>42</sup> However, single crystals became attractive for the underwater acoustic applications only after the discovery of the exceptionally high piezoelectric properties of PZN-PT solid solutions. The single crystals of the relaxor- $\text{PbTiO}_3$  solid solutions PMN-PT and PZN-PT have been the piezoelectric crystals of interest in recent decades because of their exceptional electromechanical performance. As the name implies, single crystals are materials with continuous crystalline structures. Thus, compared to their ceramic forms, single crystals are free of microstructural issues such as porosity and grain size that are intrinsic to polycrystalline ceramics. Due to lack of clamping of ferroelectric domains by grain boundaries as in ceramics, ferroelectric single crystals have lower coercive field than ceramics, typically just 1.5–7.2 kV/cm (compared to 5–30 kV/cm for PZT ceramics),<sup>44,45</sup> which makes them fairly easy to polarize and depolarize. They can be polarized much more efficiently than ceramics and thus possess extremely high piezoelectric properties, especially with the compositions near the MPBs. Figure 5 shows the phase diagrams of the two most important piezoelectric single crystal

systems, showing the MPBs of ~33%PT for PMN-PT and ~10%PT for PZN-PT. Their electromechanical coupling factor  $k_{33}$  can be greater than 0.90 (compared to about 0.7 for Navy Type 6 PZT ceramics), and the piezoelectric coefficient  $d_{33}$  can be larger than 1200 pC/N (compared to 600–700 for Navy Type 6 PZT ceramics). Under a high electric field, PZN-8%PT can even exhibit an ultrahigh piezoelectric coefficient ( $d_{33}$ ) greater than 2500 pC/N due to a field-induced rhombohedral to tetragonal (R–T) phase transition. A high coupling factor allows a transducer made from a single crystal to possess a broad bandwidth.<sup>9</sup> In sound projectors, single crystals can provide bandwidths almost triple that offered by PZT ceramics.<sup>34</sup> For example, it was shown that a PZN-PT single crystal rod-shaped transducer possessed a near 100% bandwidth, whereas that of a Navy Type 6 PZT transducer of the same geometry was only 30%.<sup>34</sup> With their piezoelectric coefficients 6–7 times those of PZT, an enhancement of 10–15 dB in source level can be achieved, or, alternatively, a 10–15 dB lower drive voltage is required for the same source level.<sup>46</sup> Piezoelectric single crystals also have Young's moduli that are 70–80% lower than the ceramics, permitting smaller transducer sizes than PZT at a given frequency range. Table 2 lists the dielectric and piezoelectric properties of PMN-PT and PZN-PT single crystals with different orientations compared to those of Navy Type 6 PZT ceramics.

The most common methods of growing commercial piezoelectric single crystals are the Bridgman method and the conventional flux method. In the Bridgman method, a vertically mounted tubular furnace with large temperature gradient (20–40°C/cm) along its axial direction is utilized.<sup>47, 48</sup> A ceramic ingot of the crystal to be grown is melted in a sealed Pt crucible in the high temperature zone of the furnace where the temperature is above the material's melting point. A seed crystal is positioned in the temperature zone where the temperature is below the melting point of the material. The crucible is slowly lowered through the furnace so the ceramic

charge is gradually exposed to the temperature gradient. Therefore, starting from the cooler end, the molten ceramic slowly crystallized from the seed crystal as it is moved through the furnace. Although this process takes days or weeks to complete, crystals as large as 10 cm in diameter and 20 cm in length can be grown by this method.<sup>48</sup> Commercial PMN-PT single crystals have been fairly successfully grown using this method. It is worth noting that compositional variation (thus property variation) caused by the segregation of  $\text{PbTiO}_3$  is a common issue for PMN-PT crystals grown by the Bridgman method. To address this problem, a Zone Melting Bridgman technique is used, in which the ceramic charge is melted only a portion at a time to prevent convection flow within the melt, thus minimizing the extent of chemical segregation along the axial direction of the crystal boule.<sup>48</sup>

In the flux method, the constituents of the crystal are mixed with a flux (typically  $\text{PbO}$  or  $\text{PbO-B}_2\text{O}_3$  mixture) in a sealed Pt crucible.<sup>47, 49-52</sup> The mixture is heated to  $1200-1260^\circ\text{C}$ <sup>47, 51, 53</sup> to form a melt and the constituents are dissolved in the flux. The mixture is then subsequently cooled at a slow cooling rate of  $0.4-2.5^\circ\text{C}/\text{hour}$ <sup>49, 51, 53, 54</sup> to promote the crystallization via supersaturation. In order to grow large crystals, local cooling must be introduced to minimize the number of spontaneous nuclei in the melt, which is usually realized by using a thin metal rod or a controlled oxygen flow at the bottom of the crucible. In this method, crystal growth starts at a relatively lower temperature than what is required in a melt growth technique, such as the Bridgman method. Therefore, the flux method is used for growing crystals that are unstable at the melting temperature or whose constituents melt incongruently, such as PZN-PT.<sup>47</sup>

Piezoelectric single crystals are largely used in naval sonar applications, where they will experience high hydrostatic pressure and/or high driving field. For hydrophone applications, one may not need to be concerned much about the small coercive fields of single crystals because

these are low-field applications. However, in deepwater sound projectors, small coercive fields become a critical concern because the transducer is usually driven by a very large alternating electric field. To prevent single crystals from becoming depolarized by either the alternating high driving field or high pressure cycling, a DC electric bias with the same polarity as that of the single crystal must be used. In addition, because the most commonly used piezoelectric single crystals, PMN-PT and PZN-PT, are both strongly electrostrictive and show a nonlinear characteristic in their strain-E field curves, a DC bias also allows the single crystal transducer to have a steady strain superimposed onto the alternating strain caused by the drive signal, resulting in more linear operation.

In addition to an electric bias, in many sonar projectors that operate in the 33-length extensional mode, a compressive mechanical pre-stress of 7 to 63 MPa on the single crystal is often used to prevent excessively large tension that may damage the material.<sup>55</sup>

Relatively low depolarization temperature is another factor that one must consider when designing a high-drive sound projector. Although relaxor ferroelectrics lose piezoelectricity only after the temperature is raised above their  $T_m$ s (around 140–150°C), depolarization actually begins around the rhombohedral–tetragonal phase transition temperature ( $T_d$ ), which is merely 70 to 95°C. Depolarization results in significantly decreased performance as the piezoelectric coefficient of a ferroelectric material is directly related to its remnant polarization by the following relationship:

$$d_{ij} = 2Q_{ij}K\varepsilon_0P_i \quad (2)$$

where  $Q_{ij}$  is the electrostriction coefficient,  $K$  the dielectric constant,  $\varepsilon_0$  the permittivity of free space, and  $P_i$  the remnant polarization. The first subscript  $i$  indicates the direction of the

polarization generated under the applied electric field, and the second subscript  $j$  indicates the direction of the induced strain.

Figure 6 shows the positions of these characteristic temperatures and polarization as a function of temperature for PMN,<sup>8</sup> showing that the polarization of the material drops quickly near  $T_d$ . The  $T_d$  for various compositions of PMN-PT and PZN-PT can also be identified in their respective phase diagrams in Figure 5 by drawing an imaginary vertical line at the corresponding composition across the MPB. This information emphasizes that when selecting the drive voltage level and the composition of the single crystal for a transducer, it is important to keep  $T_d$  in mind. During the last decade, research efforts have been made to increase the  $T_d$ s and  $E_c$ s of relaxor-PT single crystal materials. Single crystals of newer relaxor-PT systems, such as  $\text{Pb}(\text{In}_{1/2}\text{Nb}_{1/2})\text{O}_3$ - $\text{Pb}(\text{Mg}_{1/3}\text{Nb}_{2/3})\text{O}_3$ - $\text{PbTiO}_3$  (PIN-PMN-PT),  $\text{Pb}(\text{Yb}_{1/2}\text{Nb}_{1/2})\text{O}_3$ - $\text{PbTiO}_3$  (PYNT) and  $\text{BiScO}_3$ - $\text{PbTiO}_3$  (BSPT), have been developed, which possess  $T_d$ s ranging from 100°C to 350°C.<sup>56</sup>

Because of the continuous lattice structure, another distinguishing characteristic of single crystals is their high anisotropy. Their mechanical, dielectric, and piezoelectric properties can vary significantly in different orientations. Therefore, piezoelectric single crystals need to be poled and cut along specific crystallographic directions considering the manners in which the crystals will be used (e.g., 33 mode, 31 mode). In Table 2, the large differences in the dielectric and piezoelectric properties for PMN-PT and PZN-PT with different orientations are shown. In some cases, for example, in PZN-8%PT, when a large bias is applied along the  $\langle 001 \rangle$  direction of the crystal, ultrahigh large strain values ( $>1\%$ ) can be achieved by means of an electric-field-induced rhombohedral to tetragonal phase transition, showing an ultrahigh piezoelectric coefficient  $d_{33}$  of 2500 pC/N. The mechanism of this phase transition is explained in Figure 7, where one can see that at a critical value, the high electric field along the  $\langle 001 \rangle$  direction forces

the polar axes of the rhombohedral phase to collapse into the  $\langle 001 \rangle$  direction, resulting in an induced tetragonal phase and an abrupt enhancement of  $d_{33}$  (derived from the slope of the strain-E field curve).

As explained above, an induced phase transition is an effective technique for achieving exceptionally large strain in single crystals. In addition to a large electric bias, in materials such as the ternary solid solution of PIN-PMN-PT, a reversible rhombohedral to orthorhombic phase transition can be induced by compressive stress that is larger than a critical stress  $\sigma_{R-O}$ .<sup>57, 58</sup> By pre-stressing the single crystal compressively at a level close to the  $\sigma_{R-O}$  combined with a DC bias field, only a relatively small drive field ( $<1$  kV/cm) is required to induce the phase transition and achieve a strain level of  $\sim 0.5\%$ .<sup>59</sup>

The high anisotropy of the relaxor-PT single crystals is also exhibited by their significantly different  $Q_m$ s when poled in different crystallographic directions due to the mechanical loss of the non- $180^\circ$  ferroelectric domains in the material.<sup>56</sup> For example, the  $Q_m$  of  $\langle 111 \rangle$ -oriented PMN-26%PT single crystal was reported to be 2200 whereas that of the  $\langle 001 \rangle$ -oriented crystals was merely 150.<sup>60</sup>

Crack propagation resulting from anisotropy of the material is an important consideration when designing transducers to be used under conditions of high static pressure. Due to the strong anisotropy of single crystals, the internal stress caused by the poling process leads to flexural strength difference in different crystallographic directions. For instance, under DC electric fields,  $\langle 001 \rangle$  poled PMN-PT single crystals exhibit significantly more cracks and crack growth than  $\langle 011 \rangle$  poled crystals. Therefore, a compressive pre-stress may be needed for  $\langle 011 \rangle$  poled PMN-PT crystals to suppress crack initiation and propagation.<sup>46</sup>

The biggest disadvantage of piezoelectric single crystals compared with piezoelectric ceramics is their significantly higher cost, due to the difficulty of growing large crystals with few defects.<sup>61</sup> This is the main barrier preventing single crystals from replacing PZT ceramics for many applications. In addition, currently, the maximum single crystal size that can be grown is 10 cm in diameter and 20 cm in length,<sup>47</sup> which limits the dimensions of the transducers which can be produced using single crystals.

Both theoretical and experimental studies of single-crystal-based underwater acoustic projectors have demonstrated that PMN-PT and PZN-PT can provide markedly higher voltage response with much smaller hysteresis permitting for smaller and lighter transducer designs than PZT ceramics.<sup>62-67</sup> Single crystal manufacturers have been striving to reduce the production cost of these crystals<sup>48</sup> and the cost of the active material is only a portion of the total cost of an acoustic transmitter. Depending upon the nature of the acoustic transmitter the use of the less costly PZT ceramic elements may not translate to a price advantage over single crystals because of the higher design cost required when an electromechanically inferior material is used.<sup>68</sup>

## **5. PIEZOELECTRIC POLYMERS**

Piezoelectric ceramics and single crystals offer excellent piezoelectric activity because of their strong ferroelectric properties. After PZT was discovered, PZT ceramics became widely used in underwater transducers because they offer a great compromise between manufacturing cost and performance. Single crystals are used in the applications where ultra-high sensitivity and acoustic power are needed. However, both of these materials have characteristics that are not ideal for certain underwater transducer applications.



The first is high acoustic impedance. Both single crystals and ceramics have very high acoustic impedance, which is defined as the product of the material density and the sound velocity in the material, because of their high densities and elastic moduli. The typical acoustic impedance of piezoelectric ceramics and single crystals is greater than 30 MRayls [ $10^6 \text{g}/(\text{m}^2\text{s})$ ], whereas that of water is only 1.5 MRayls. Such a large acoustic impedance mismatch causes significant reflection of the acoustic signal at the interface between the material and water. Therefore, for underwater applications acoustic matching layers are required for piezoelectric ceramics and single crystals.

Second is their low hydrostatic piezoelectric response. In hydrophone applications where acoustic energy is converted into electric energy, the piezoelectric voltage constant  $g$  of the piezoelectric material directly relates to the hydrophone sensitivity as it expresses the electric field generated in the material per unit of mechanical stress applied. The hydrostatic piezoelectric voltage constant  $g_h$  is related to the  $g$  coefficients of other operational modes by the following equation

$$g_h = g_{33} + g_{32} + g_{31} \quad (3)$$

where  $g_{33}$  is the thickness mode in the poled direction of the materials, and  $g_{32}$  and  $g_{31}$  are the in-plane modes that describes the material response when the stress is applied perpendicular to the poled direction. For piezoelectric ceramics,  $g_{32}$  and  $g_{31}$  are negative while  $g_{33}$  is positive, resulting in a very small  $g_h$ . Another frequently used piezoelectric coefficient is the hydrostatic piezoelectric charge constant  $d_h$ , describing the generated strain per unit of electric field.  $g_h$  and  $d_h$  are related by

$$g_h = \frac{d_h}{\epsilon_0 K} \quad (4)$$

where  $K$  is the relative permittivity of the material and  $\epsilon_0$  the permittivity of free space. The product of  $g_h$  and  $d_h$  is often used as the figure of merit (FOM) for hydrophone materials.

The third disadvantage is the lack of flexibility. In many naval sonar applications, it is desired or required that the piezoelectric material be flexible so it can conform to curved surfaces. Ceramics and single crystals are hard and brittle. Complex fabrication steps are needed to have them conform to curved surfaces.

Piezoelectric polymers excel in applications where high acoustic impedance, low hydrostatic piezoelectric response, and flexibility are significant design constraints. Their low density and elastic constants translate into much lower acoustic impedance (merely two to six times that of water), thus offering much better acoustic matching with water. They also possess much better hydrostatic-mode response and are much more flexible than ceramics and single crystals. Piezoelectric polymers can also be dissolved in solutions, enabling fabrication possibilities such as spraying, spin-coating, molding, and dipping. These advantages allow piezoelectric polymers to become good active material candidates for underwater acoustic transducer materials.

PVDF was the first polymer to demonstrate relatively strong piezoelectricity. It has a chemical formula of  $(\text{CH}_2\text{CF}_2)_n$ . This polymer contains about 50% lamellar crystals that are tens of nanometers thick and up to 100 nanometers long embedded in an amorphous matrix. The structures of four different crystalline phases of PVDF are illustrated in Figure 8.<sup>22</sup> Form I, also called the  $\beta$  phase, is the most common phase that displays ferroelectricity. The non-polar  $\alpha$  phase (Form II) must be mechanically stretched or rolled, either uniaxially or biaxially, to be converted into the piezoelectric Form I. A poling step is then applied to orient the dipoles. PVDF and its copolymers such as P(VDF-TrFE), P(VDF-TeFE), and P(VDCN-VAC) are the most

common piezoelectric polymers used in underwater transducers. Among these co-polymers, P(VDF-TrFE) and P(VDF-TeFE) can directly form a polar phase (Form I) through copolymerization without the need of stretching or drawing, because the extra fluorine atoms introduced into the polymer chain by TrFE and TeFE result in steric hindrance which prevents formation of the non-polar  $\alpha$  phase.<sup>69</sup> Only poling is necessary to render the material piezoelectric.<sup>70</sup> This characteristic enable the copolymers to be dissolved in liquid solvents so that they can be extruded or molded into desired shapes or directly coated onto a substrate,<sup>71</sup> adding more flexibility in transducer design. Odd-number nylons such as Nylon-5, Nylon-7, and Nylon-11 were also piezoelectric polymers to consider for transducers because of their similar remnant polarization to that of PVDF and their very low acoustic impedance. However, their highly hydrophilic character requires special consideration for underwater transducers.<sup>72</sup> The typical underwater transducer-related properties of PVDF-based polymers are given in Table 3.<sup>71, 73</sup>

As shown in Table 3, piezoelectric polymers have disadvantages as well as advantages. The electromechanical properties of piezoelectric polymers are significantly inferior to those of ceramics. Their thickness-mode electromechanical coupling coefficient  $k_t$  is around only 0.2, less than one-half the typical value of PZT ceramics (0.4–0.5), and their  $d_{33}$  is in the range of only 10–25 pC/N, an order of magnitude lower than those of PZT. They also possess lower dielectric constants but higher dielectric loss. As shown in Table 3, in comparison with PZT ceramics, the dielectric constants of piezoelectric polymers are 2-3 orders of magnitude lower (merely 5-6) but their dielectric loss is an order of magnitude higher (12-25%). The low dielectric constants present challenges for electrical impedance matching for a transducer if the transducer electronics are not in close proximity to the material.<sup>70</sup>

The low electromechanical properties (with the exception of those for hydrostatic mode) of piezoelectric polymers limit their use in underwater transmitters. However, their excellent acoustic impedance (3-4 MRayls), low  $Q_m$  (10-25), and  $g_h$  ( $90-275 \times 10^{-3} \text{Vm/N}$ ) provide high receiving sensitivity and much flatter frequency response than ceramics, making them good candidates for hydrophone applications. For instance, the typical -6 dB fractional bandwidth of PVDF is greater than 150%, which is much larger than that of Navy Type 6 PZT ceramics (60%).<sup>74</sup> To date, PVDF-based piezoelectric polymers have been used in a wide range of hydrophones: 31 mode<sup>75</sup>, hydrostatic mode<sup>76</sup>, thickness mode<sup>77, 78</sup> as well as hydrophone arrays.<sup>79</sup> The film geometry of piezoelectric polymers also permits the fabrication of a large number of small transducers on a single silicon wafer.<sup>80, 81</sup> These integrated hydrophone arrays provide the possibility of further integrating signal-processing components on-chip. In addition, having no moving parts makes these microelectromechanical system arrays good candidates for operating in high-pressure environments.<sup>81</sup>

An additional advantage that piezoelectric polymers have over the ceramics is their better high frequency response, which allows them to be the preferred material for high-frequency applications.<sup>82</sup> Therefore, although they are not favored for low-frequency transmitting applications due to their low electromechanical properties when compared to PZT, they can still be good candidates for high-frequency transmitting applications. For example, in underwater wireless communication applications where the frequencies are in the MHz range, it has been shown that the sensitivity of a PVDF transmitter can be four times that of a Type 6 PZT transmitter.<sup>83</sup>

When piezoelectric polymers are used in transducer designs, several characteristics unique to these materials need to be considered. For instance, polymers typically have much lower melting

temperatures than ceramics. Therefore, the fired-on electroding technique widely used in piezoelectric ceramics cannot be used. Moreover, PVDF-based polymers are fluorinated and have fairly low surface energy and are highly hydrophobic.<sup>84</sup> These properties present problems for electroding as well as bonding with backing materials. Surface treatments are usually needed to overcome such problems.<sup>85</sup>

## **6. PIEZOELECTRIC COMPOSITES**

### **6.1 Connectivity Patterns of Piezoelectric Composites and Their Fabrication Methods**

As discussed in Section 5, piezoelectric ceramics and single crystals, because of their high acoustic impedance, low hydrostatic piezoelectric coefficients, and lack of flexibility, are not optimum for underwater transducer applications. Polymers, on the other hand, have acoustic impedances very close to that of water, and they are very flexible. However, their piezoelectric performance is inferior to that of ceramics and single crystals. A single-phase material that possesses both the merits offered by piezoelectric ceramics/single crystals and piezoelectric polymers simply does not exist. Thus, prior to piezoelectric composites, compromises were required in underwater transducer designs. In 1978, Newnham introduced the concept of “connectivity” in piezoelectric and pyroelectric ceramic composites<sup>10</sup> and then started to apply the idea to piezoelectric–polymer composites in the 1980s.<sup>11, 86</sup> By structurally combining a piezoelectric ceramic and a polymer with certain connectivity, the resulting composite material can successfully integrate the best of both worlds. Akdogan and Safari provided excellent reviews of piezoelectric composites used in transducers, sensors, and actuators.<sup>87, 88</sup> A graphic comparison of the FOMs of various types of piezoelectric composites compared to those of PZT

and PVDF is given in Figure 9,<sup>87, 89-94</sup> demonstrating dramatic enhancement of FOM offered by composites.<sup>87</sup>

Connectivity defines the way in which the two end members (the piezoelectric ceramic and the polymer) connect in the composite. Mathematically, there are 10 different ways in which the two phases are connected in a two-phase composite, which are described by two numbers (e.g., 0-3, 1-3).<sup>10</sup> Each digit describes the number of dimensions in which an individual phase is connected. The convention is that the first digit defines how the active ceramic (the piezoelectric) is connected and the second how the passive phase (the polymer) is connected.<sup>88</sup> For example, a 0-3 composite is fabricated by dispersing isolated piezoelectric ceramic particles (hence “0” dimensional) in a polymer matrix (hence “3” dimensional). A 1-3 composite is an array of piezoelectric ceramic rods embedded in a polymer with electrodes at the rod ends. To date, commercial piezoelectric composite transducers are primarily 0-3, 1-3, and 2-2 composites. Figure 10 illustrates the typical connectivity patterns of these three types of composites.

The most common methods of fabricating piezoelectric composites include dice and fill, lost mold, injection molding, tape casting and extrusion. The dice and fill method is a simple technique used to make 1-3 and 2-2 composites. With dice and file, a 2-2 composite is made from a solid block of sintered piezoelectric ceramic with a series of parallel cuts (without cutting through the whole specimen) in one direction followed by filling the cuts with the polymer. The first step in making a 1-3 composite, is the same set of parallel cuts needed for a 2-2 composite followed by rotating the block by 90° and making a second series of parallel cuts to form the ceramic rods, followed by filling the spaces between rods with the polymer. One obvious disadvantage of the dice and fill method is the waste of material inherent to the dicing process. The 2-2 composites can also be made using the tape casting method, in which thin sheets of PZT

and polymers are cast and then stacked together.<sup>95</sup> This method can provide transducers that operate at very high frequencies, determined primarily by the thickness of the tapes. Tape casting and dice and fill can be combined to produce 1-3 composites by dicing the stacked tapes. In the lost mold method, the desired ceramic structure is defined by a plastic mold, which is filled with PZT slurry. During a drying stage the plastic mold is burned (hence “lost”).<sup>96</sup> This process can provide complex structures, such as honeycomb-shaped rods, which are quite difficult to obtain with dice and fill. Injection molding is used to produce composites with complex structures at fine scales (<40- $\mu\text{m}$  feature size), in this method, a ceramic paste is injected into a mold to form the desired structure, solidified, and then ejected from the mold. The advantages of injection molding include the flexibility of structure design, low cost, and low material waste. For structures with even finer feature size (<20  $\mu\text{m}$ ), such as those requiring microfabrication, co-extrusion can be used.<sup>97</sup> This method involves repetitive extrusion of ceramic–plastic feed rods that have the feature shape. The extrusion apparatus contains a size-reduction cone that incrementally reduces the cross-sectional area of the feed rods in each step of extrusion (the feed rods become longer after extrusion). During the first extrusion, only one feed rod is used. The longer extruded rod is then cut into smaller pieces, each of which contains the same feature as the initial feed rod, and then reassembled together and extruded again. Repeating the extrusion–reassembly cycles causes the feature size to become smaller and smaller, down to  $\sim 10\text{-}\mu\text{m}$  range. In recent years, as computer technology advanced, computer-aided design (CAD) is used more frequently in composite fabrication, yielding a new branch of fabrication methods called solid freeform fabrication (SFF). Three-dimensional printing is one example.<sup>98</sup> Using this method, a SFF manufacturing machine fabricates the structure of a composite layer by layer (slice by slice) based on a slice file converted from a CAD file that contains the design detail for the composite.

Thanks to layer-by-layer fabrication and the degree of structure complexity that a CAD file can deliver, SFF methods are rapid and capable of producing complex structures that are not feasible with other techniques.

## 6.2 0-3 Composites

The main advantage of 0-3 composites is the simplicity with which they can be fabricated in large sizes and various geometries, such as sheets, bars and fibers. Although the 0-3 connectivity pattern is fairly simple, it is difficult to uniformly distribute the ceramic particles in the polymer matrix, especially at high solid loadings. Because of the presence of surface charge, ceramic particles without surface modification tend to agglomerate, resulting in deviation from the intended zero-dimensional connectivity. Agglomeration also creates voids between the particles, which lowers the dielectric breakdown strength of the composite, limiting the voltage that can be applied to the composite during the poling process. The first 0-3 piezoelectric composites were produced before the concept of connectivity was introduced and used in production of composites. Early 0-3 composites displayed relatively low FOMs in the range of  $1000\text{--}5000 \times 10^{-15} \text{ m}^2/\text{N}$ .<sup>87</sup> Han developed a colloidal processing method for  $0.5\text{PbTiO}_3\text{-}0.5\text{Bi}(\text{Fe}_{0.98}\text{Mn}_{0.02})\text{O}_3$  (PT-BF) that utilized a polymer coating to overcome the agglomeration problem. The FOM of the composite was enhanced to  $6000 \times 10^{-15} \text{ m}^2/\text{N}$ .<sup>99</sup> In 0-3 composites, the FOM can also be affected by the particle size of the ceramic and the density. Smaller particle size provides lower  $d_h$  values and FOM that is independent of pressure; with larger particle size, higher  $d_h$  values can be achieved, but the FOM displays a certain degree of dependence on pressure, due to the formation of voids, the result of using large particles.<sup>100-102</sup>

## 6.3 1-3 Composites



A 1-3 piezoelectric composite consists of parallel piezoelectric ceramic rods separated by a polymer phase. In a piezoelectric composite, the volume average of the hydrostatic pressure-induced electric displacement is expressed by the following equation:<sup>103, 104</sup>

$$D_z = d_{31}T_{rr} + d_{31}T_{\theta\theta} + d_{33}T_{zz} + \varepsilon_{33}^T E_z \quad (5)$$

where  $\varepsilon_{33}^T$  is the permittivity of the piezoelectric ceramic,  $E_z$  is the electric field, and the  $T_{ij}$  are the stress components induced in the rod. The hydrostatic piezoelectric constant  $d_h$  of the composite is given by

$$d_h = \frac{-D_z}{p} \quad (6)$$

where  $p$  is the pressure. From equations 5 and 6, it is evident that for a 1-3 piezoelectric composite, it is desirable to increase the axial stress (stress amplification) or reduce the lateral stress in the piezoelectric ceramic rods to improve electromechanical coupling. Ideally, the polymer phase should exhibit good stress amplification due to its more compliant nature. However, the polymer's high Poisson's ratio creates opposing stress to the applied stress, reducing stress amplification. Thus, the enhancement of  $d_h$  is not as much as expected.<sup>87, 88, 105</sup> Several methods have been implemented to counteract the high Poisson's ratio of the polymer to increase stress amplification, including introduction of pores into the polymer<sup>105</sup> and addition of stiff glass fibers in the transverse direction of the rods to provide transverse reinforcement<sup>106</sup>, and separating the polymer and ceramic rods in the lateral direction<sup>107</sup>. The enhancement of electromechanical coupling by stress amplification in 1-3 composites can be readily seen in their FOMs shown in Figure 9.

When used in 2-dimensional high-density arrays, 1-3 piezoelectric composites can be fabricated into a multilayer structure, in which the piezoelectric rods of different layers are electrically connected in parallel, to minimize the undesirably high electrical impedance. In this case, the alignment of piezoelectric rods between the adjacent layers becomes critical as rod misalignment results in extraneous thickness modes. Simulation and Experimental analyses have shown that a 15% of rod misalignment between layers is the critical point where extraneous modes appear.<sup>108, 109</sup>

#### **6.4 2-2 Composites**

2-2 composites are stacks of piezoelectric ceramic sheets separated by polymer layers. They are usually used at ultrasonic frequency ranges within the thickness mode of the ceramic layers. Therefore, the thickness electromechanical coupling coefficient  $k_t$  is the most important parameter for these materials. To maximize the effective  $k_t$  of the composite, the thickness-mode resonance must be decoupled from the planar mode. This can be achieved by two methods. The first is to increase the thickness/width aspect ratio of the piezoelectric layers. Obviously, a small  $t/w$  aspect ratio results in a small  $k_t$ . It has been determined that when the aspect ratio is greater than 4, the decrease in  $k_t$  becomes negligible.<sup>88, 110</sup> The second method is to introduce a third phase in the form of a filler powder, such as glass spheres, alumina, or zirconia, into the polymer layer to form a 2-0-2 composite (the second digit denotes the connectivity of the filler powder) to change the Poisson's ratio of the composite and its lateral resonance.<sup>111</sup>

In addition to the decoupling of thickness and lateral resonance modes, the fashion in which the layers are oriented with respect to the poling directions of piezoelectric phases is also important. For hydrophone applications, the theoretical study conducted by Challagulla and

Venkatesh has shown that the best transducer properties can be obtained in longitudinally layered ceramic-polymer 2-2 thin film composites.<sup>112</sup>

## 6.5 Moonie and Cymbal Transducers

It is worth mentioning that the non-piezoelectric phase in piezoelectric composites can also be air. It is not necessary that it always be a polymer. A piezoelectric–air composite was derived from the concept of “Moonie” actuators.<sup>113</sup> In a Moonie actuator, a metal (usually brass because of its relatively small thermal expansion coefficient) end cap with a thin air cavity is bonded onto each side of a piezoelectric ceramic disc. When the piezoelectric disc is excited, the radial motion of the ceramic induces the flextensional motion of the end caps. The resulted axial displacement is added to the displacement caused by the 33 mode of the piezoelectric ceramic itself, thus amplifying the axial displacement. As a result, the effective piezoelectric coefficient  $d_{33}$  is greatly enhanced. Because  $d_h = d_{33} + 2d_{31}$ , an enhanced  $d_h$  is achieved. Moreover, because of the air cavities, the acoustic impedance of the entire composite is also significantly reduced, enabling an improved acoustic impedance matching with water. These two effects significantly improve the FOM of Moonie composites. As shown in Figure 9, Moonie composites exhibit a very high FOM, reaching  $50000 \times 10^{-15} \text{ m}^2/\text{N}$ .<sup>92</sup> Not long after the Moonie design was introduced, an improved design with a shape resembling a cymbal emerged. The main difference between the Cymbal design and the Moonie design is the structure of the metal endcaps. A Cymbal transducer utilizes thinner metal endcaps that have a slightly different shape to remove most of the stress concentration in the endcaps so as to achieve higher and more reproducible displacement.<sup>114</sup> The result of this improved design is an excellent FOM that could be as high as  $10^6 \times 10^{-15} \text{ m}^2/\text{N}$ .<sup>94</sup>

An intrinsic problem of the Cymbal design is the splitting of resonance frequency resulted from the inevitable small differences (variation in weight, size and bonding) in the two metal caps.<sup>115</sup> Resonance frequency splitting results in lower efficiency of the transducer, and thus is not desirable. It can be solved by adding external mass to the endcaps, or filling (or partially filling) the air cavity with liquid.<sup>116</sup> In addition, a limitation of the traditional Cymbal design is the pressure resistance of the transducer, as the endcaps tend to collapse when experiencing high pressure (200-meter deep water or 2 MPa).<sup>117</sup> An innovative design to overcome this limitation is to use a “double-dipper” design, in which piezoelectric ceramic rings instead of discs are used combined with concave metal endcaps. This design allows for an operation pressure up to 6 MPa without significant property degradation.<sup>117, 118</sup>

When used in underwater sound projectors, Cymbal transducers are usually incorporated into arrays because a single Cymbal transducer possesses a high  $Q_m$  and low efficiency due to its small dimension with respect to the wavelength in water.<sup>117</sup>

## **6.6 Single Crystal Composites**

Because the piezoelectric properties of relaxor-PT ferroelectric single crystals are far superior to those of piezoelectric ceramics, in the last decade, application of single crystals in piezoelectric composites has started to be explored both theoretically and experimentally for 1-3 and 2-2 composites. Simulation has shown that a sonar array consisting of PMN-32%PT single crystal 1-3 composite elements could offer an enhancement of 2–4 dB in transmission and reception over Navy Type 6 PZT ceramics.<sup>119</sup> Experiments have been conducted where 1-3 composites prepared with both PMN-PT and PZN-PT single crystals were fabricated and their properties compared with Navy Type 6 PZT ceramic composites in similar configurations. The

results have shown greater FOMs and  $g_h$  than those of the single crystals, PZT ceramics, and PZT composites.<sup>93, 120, 121</sup>

## 7. SUMMARY

Piezoelectric materials have been used in underwater acoustic transducers for nearly a century. Lead-based materials such as PZT and relaxor ferroelectrics have dominated the field because of their excellent electromechanical properties. PZT ceramics are used most commonly in both hydrophones and sound projectors, in the form of either monolithic ceramics or composites, due to the wide variety of piezoelectric properties they offer and the ease with which they can be fabricated.

Piezoelectric polymers have much better acoustic impedance matching with water, higher hydrostatic response, and broader bandwidth than ceramics and single crystals. They also offer flexibility for fabrication of transducers in large sizes and various geometries. These advantages make them good materials for hydrophone applications. However, they have the disadvantages that their piezoelectric coefficients and dielectric constants are much lower than those of PZT ceramics and single crystals.

Relaxor-PT ferroelectric single crystals were one of the most important technological advances made in the field of underwater acoustic transducers in recent decades. They provide remarkably improved transducer performance in many aspects of acoustic transducer applications. PMN-PT and PZN-PT are the two most important piezoelectric single crystal families used in underwater transducers. They provide higher electromechanical coupling factors and a few times higher electromechanical strains than soft PZT ceramics due to their more uniform domain structure and large electrostrictive response. Exceptionally large strains could be

obtained in these materials by inducing ferroelectric phase transitions through either an electric bias or an applied stress. They have been used mainly in sound projectors where high acoustic power and broad bandwidth are required. The disadvantages of relaxor-PT ferroelectric single crystals include low depolarization temperature and coercive field, and the high cost of these single crystals. New relaxor-PT systems with higher depolarization temperature have been developed. In the last 15 years, continuous development efforts have also been made to reduce the manufacturing cost of the single crystals to make the use of these materials more practical. Although it is highly unlikely that the cost of single crystals becomes competitive with that of ceramic materials because of the inherent complexity of their growth processes, the continuously reduced cost will allow them to be used in a wider range of acoustic applications where only ceramics have been used.

Piezoelectric composites combine the advantages of both piezoelectric ceramics and polymers by incorporating them with certain connectivity patterns using various fabrication methods. These materials can be used as sound projectors as well as receivers. This approach allows piezoelectric ceramics and single crystals to achieve improved hydrostatic response while gaining better acoustic impedance matching with water. As a result, significantly higher figures of merit can be achieved with piezoelectric composites than with single-phase piezoelectric materials. Therefore, in the last 10 years, a majority of piezoelectric material studies for underwater acoustic applications have been conducted on piezoelectric composites. However, most of the research work has been focused on the combination of piezoelectric ceramics and polymer materials. Piezoelectric properties of the ceramic components in piezoelectric composites largely determine the performance ceiling of piezoelectric composite transducers. Studies on single crystal-polymer composites are still relatively scarce. We believe that as the

cost of single crystals continues to decline and crystals with larger sizes become available, it is conceivable that piezoelectric single crystals will be increasingly adopted in composites materials for further improvement in transducer performance.

In summary, in the near future, lead-base ferroelectric ceramics and their composites will continue to dominate the field of underwater acoustic transducers because of their low cost, excellent performance and the wide range of available sizes and geometries. For hydrophone applications, piezoelectric polymers are also good candidates due to their excellent hydrostatic properties and acoustic impedance matching with water. As new materials emerge and the manufacturing processes improve, relaxor-PT ferroelectric single crystals will see increasing use as either monolithic elements or the active components of composites in underwater acoustic transducers.

## **ACKNOWLEDGEMENTS**

The work described in this article was funded by the U.S. Army Corps of Engineers, Portland District. Brad Eppard is the technical lead for the USACE, and we greatly appreciate his leadership and support of this research. The authors are grateful also to many staff of the Pacific Northwest National Laboratory for their technical help—including Tylor Abel, Duane Balvage, Samuel Cartmell, Honghao Chen, Andrea Currie, Jayson Martinez, Mitchell Myjak, Jie Xiao, and Yong Yuan. The study was conducted at PNNL, operated in Richland, Washington, by Battelle for the U.S. Department of Energy.

## REFERENCES

1. C. H. Sherman and J. L. Butler, in *Transducers and Arrays for Underwater Sound*, R. R. Goodman, H. P. Bucker, I. Dyer and J. A. Simmen, Springer Science+Business Media, LLC, New York (2007) pp.76-212
2. B. Jaffe, R. S. Roth, and S. Marzullo, *J. Appl. Phys.*, 25, 809, (1954)
3. S. Fushimi and T. Ikeda, *J Am Ceram Soc*, 50, 129, (1967)
4. R. Clarke and R. W. Whatmore, *J. Cryst. Growth*, 33, 29, (1976)
5. J. Kuwata, K. Uchino, and S. Nomura, *Jpn. J. Appl.Phys.*, 21, 1298, (1982)
6. S. Saitoh, M. Izumi, S. Shimanuki, S. Hashimoto, and Y. Yamashita, Patent No. 5295487, USPTO, (1994)
7. T. R. Shrout, Z. P. Chang, N. Kim, and S. Markgraf, *Ferroelectrics Lett.*, 12, 63, (1990)
8. T. R. Shrout and J. Fielding, *IEEE 1990 Ultrasonics Symposium: Proceedings, Vols 1-3*, 711, (1990)
9. S. E. Park and T. R. Shrout, *IEEE Transactions on Ultrasonics Ferroelectrics and Frequency Control*, 44, 1140, (1997)
10. R. E. Newnham, D. P. Skinner, and L. E. Cross, *Mater. Res. Bull.*, 13, 525, (1978)
11. R. E. Newnham, L. J. Bowen, K. A. Klicker, and L. E. Cross, *Materials & Design*, 2, 93, (1980)
12. T. A. Ford and W. E. Hanford, Patent No. 2435537, USPO, (1948)
13. H. Kawai, *Jpn. J. Appl.Phys.*, 8, 975, (1969)
14. A. J. Holden, A. D. Parsons, and A. E. J. Wilson, *J. Acoust. Soc. Am.*, 73, 1858, (1983)
15. E. F. Carome, G. R. Harris, and A. S. de Reggi, *J. Acoust. Soc. Am.*, 64, S56, (1978)
16. M. A. Josserrand and C. Maerfeld, *J. Acoust. Soc. Am.*, 78, 861, (1985)



17. B. Jaffe, J. William R. Cook, and H. Jaffe, in *Piezoelectric Ceramics*, Academic Press Limited, (1971)
18. T. Furukawa, IEEE Trans. Electr. Insul., 24, 375, (1989)
19. T. Furukawa, Phase Transit., 18, 143, (1989)
20. G. Gerliczy and R. Betz, Sens. Actuators, 12, 207, (1987)
21. Y. Takase, J. W. Lee, J. I. Scheinbeim, and B. A. Newman, Macromolecules, 24, 6644, (1991)
22. G. M. Sessler, J. Acoust. Soc. Am., 70, 1596, (1981)
23. J. A. Gallegojuarez, J. Phys. E: Sci. Instrum., 22, 804, (1989)
24. *Piezoelectric Ceramic Material and Measurements Guidelines for Sonar Transducers*, MIL-STD-1376B (SH), U.S. Department of Defense, (1995)
25. L. M. Levinson, in *Electronic Ceramics (Electrical and Computer Engineering)*, CRC Press, (1987)
26. G. A. McMichael, M. B. Eppard, T. J. Carlson, J. A. Carter, B. D. Ebberts, R. S. Brown, M. Weiland, G. R. Ploskey, R. A. Harnish, and Z. D. Deng, Fisheries, 35, 9, (2010)
27. M. A. Weiland, Z. D. Deng, T. A. Seim, B. L. LaMarche, E. Y. Choi, T. Fu, T. J. Carlson, A. I. Thronas, and M. B. Eppard, Sensors, 11, 5645, (2011)
28. Z. D. Deng, M. A. Weiland, T. Fu, T. A. Seim, B. L. LaMarche, E. Y. Choi, T. J. Carlson, and M. B. Eppard, Sensors, 11, 5661, (2011)
29. M. B. Moffett, M. D. Jevnager, S. S. Gilardi, and J. M. Powers, J. Acoust. Soc. Am., 105, 2248, (1999)

- 30.** G. Yang, S. F. Liu, W. Ren, and B. K. Mukherjee, in *Uniaxial stress dependence of the piezoelectric properties of lead zirconate titanate ceramics*, C. S. Lynch, Ed., Spie-Int Soc Optical Engineering, Bellingham (2000), Vol. 3992, p.103-113.
- 31.** R. S. L. Fisher, E. A. McLaughlin, and H. C. Robinson, in *Stress dependent behavior of  $d_{33}$  and  $Y_{33}^E$  in navy type III and VI ceramics*, C. S. Lynch, Ed., Spie-Int Soc Optical Engineering, Bellingham (2002), Vol. 4699, p.522-531.
- 32.** L. E. Cross, *Ferroelectrics*, 76, 241, (1987)
- 33.** J. F. Tressler, in *Piezoelectric and Acoustic Materials for Transducer Applications*, Edited by A. Safari and E. K. Akdogan, Springer Science+Business Media, LLC, New York (2008), Chapter 11, pp. 224
- 34.** K. Uchino, in *Advanced Piezoelectric Materials - Science and Technology*, Edited by K. Uchino, Woodhead Publishing, Philadelphia (2010), Chapter 1, pp. 33
- 35.** E. Ringgaard and T. Wurlitzer, *J. European Ceram. Soc.*, 25, 2701, (2005)
- 36.** J. Rödel, W. Jo, K. T. P. Seifert, E.-M. Anton, T. Granzow, and D. Damjanovic, *J Am Ceram Soc*, 92, 1153, (2009)
- 37.** Y. Saito, H. Takao, T. Tani, T. Nonoyama, K. Takatori, T. Homma, T. Nagaya, and M. Nakamura, *Nature*, 432, 84, (2004)
- 38.** R. C. Turner, P. A. Fuierer, R. E. Newnham, and T. R. Shrout, *Appl. Acoust.*, 41, 299, (1994)
- 39.** J. T. Luo, X. Y. Zhu, G. Chen, F. Zeng, and F. Pan, *Physica Status Solidi-Rapid Research Letters*, 4, 209, (2010)
- 40.** F. Xu, R. A. Wolf, T. Yoshimura, and S. Trolier-McKinstry, in *Piezoelectric films for MEMS applications*, R. J. Fleming, (2002)
- 41.** F. Pan, J. Luo, Y. Yang, X. Wang, and F. Zeng, *Sci. China-Technol. Sci.*, 55, 421, (2012)

42. S. Tadigadapa and K. Mateti, *Meas. Sci. Technol.*, 20, (2009)
43. Q. Zhou, S. Lau, D. Wu, and K. Kirk Shung, *Progress in Materials Science*, 56, 139, (2011)
44. H. Chen and R. Panda, in *Review: Commercialization of piezoelectric single crystals for medical imaging applications*, Ed., (2005), Vol. p.235-240.
45. J. J. Bernstein, S. L. Finberg, K. Houston, L. C. Niles, H. D. Chen, L. E. Cross, K. K. Li, and K. Udayakumar, *IEEE Transactions on Ultrasonics Ferroelectrics and Frequency Control*, 44, 960, (1997)
46. L. M. Ewart, E. A. McLaughlin, H. C. Robinson, J. J. Stace, and A. Amin, *IEEE Transactions on Ultrasonics Ferroelectrics and Frequency Control*, 54, 2469, (2007)
47. S. Zhang and F. Li, *J. Appl. Phys.*, 111, 031301, (2012)
48. P. W. Rehrig, W. S. Hackenberger, J. Xiaoning, T. R. Shrout, Z. Shujun, and R. Speyer, 2003 *IEEE Symposium on Ultrasonics*, 1, 766-769, (2003)
49. K. Harada, S. Shimanuki, T. Kobayashi, Y. Yamashita, and S. Saitoh, *J Am Ceram Soc*, 85, 145, (2002)
50. T. Sekiya, K. Kusumoto, H. J. Hwang, J. P. Reyes, J. P. Chaminade, and J. Ravez, *Journal of the Korean Physical Society*, 32, S1201, (1998)
51. T. Kobayashi, S. Saitoh, K. Harada, S. Shimanuki, and Y. Yamashita, *Applications of Ferroelectrics*, 1998. ISAF 98. Proceedings of the Eleventh IEEE International Symposium on, 235-238, (1998)
52. B. Srimathy, R. Jayavel, A. Thamizhavel, and J. Kumar, *AIP Conference Proceedings*, 1349, 119, (2011)
53. S. Saitoh, T. Takeuchi, T. Kobayashi, K. Harada, S. Shimanuki, and Y. Yamashita, *IEEE Trans. Ultrason. Ferroelectr. Freq. Control*, 46, 414, (1999)

- 54.** B. Srimathy, R. Jayavel, S. Ganesamoorthy, I. Bhaumik, A. K. Karnal, V. Natarajan, E. Varadarajan, and J. Kumar, *Crystal Research and Technology*, 1, **(2012)**
- 55.** A. Amin, E. McLaughlin, H. Robinson, and L. Ewart, *IEEE Transactions on Ultrasonics Ferroelectrics and Frequency Control*, 54, 1090, **(2007)**
- 56.** S. Zhang and T. R. Shrout, *IEEE Trans. Ultrason. Ferroelectr. Freq. Control*, 57, 2138, **(2010)**
- 57.** A. Amin and L. E. Cross, *J. Appl. Phys.*, 98, **(2005)**
- 58.** C. Okawara and A. Amin, *Appl. Phys. Lett.*, 95, **(2009)**
- 59.** P. Finkel, K. Benjamin, and A. Amin, *Appl. Phys. Lett.*, 98, **(2011)**
- 60.** S. Zhang, N. P. Sherlock, J. Richard J. Meyer, and T. R. Shrout, *Appl. Phys. Lett.*, 94, 162906, **(2009)**
- 61.** C. G. Oakley and M. J. Zipparo, in *Single crystal piezoelectrics: A revolutionary development for transducers*, S. C. Schneider, M. Levy and B. R. McAvoy, Ed., IEEE, New York **(2000)**, Vol. 1 & 2, p.1157-1167.
- 62.** J. F. Tressler, T. R. Howarth, and D. H. Huang, *J. Acoust. Soc. Am.*, 119, 879, **(2006)**
- 63.** J. B. Babu, G. Madeswaran, R. Dhanasekaran, K. Trinath, A. Rao, N. S. Prasad, and I. R. Abisekaraj, *Def. Sci. J.*, 57, 89, **(2007)**
- 64.** P. W. Rehrig, W. S. Hackenberger, X. Jiang, R. J. Meyer, and X. Geng, *Smart Structures and Materials 2003: Active Materials: Behavior and Mechanics*, 5053, 445-452, **(2003)**
- 65.** P. W. Rehrig, W. S. Hackenberger, X. N. Jiang, R. J. Meyer, and X. C. Geng, in *Naval device applications of relaxor piezoelectric single crystals*, D. E. Yuhas and S. C. Schneider, Ed., IEEE, New York **(2002)**, Vol. 1 & 2, p.733-737.

66. M. B. Moffett, H. C. Robinson, J. M. Powers, and P. D. Baird, *J. Acoust. Soc. Am.*, 121, 2591, (2007)
67. J. F. Tressler and T. R. Howarth, *Proceedings of the 2000 12th IEEE International Symposium on Applications of Ferroelectrics*, 2, 561-564 vol. 2, (2000)
68. T. C. Montgomery, R. J. Meyer, and E. M. Bienert, *OCEANS 2007*, 1-5, (2007)
69. A. C. Jayasuriya and J. I. Scheinbeim, *Applied Surface Science*, 175–176, 386, (2001)
70. W. A. Smith, in *New Opportunities in Ultrasonic Transducers Emerging from Innovations in Piezoelectric Materials*, F. L. Lizzi, Spie - Int Soc Optical Engineering, Bellingham (1992)
71. L. F. Brown, in *Ferroelectric Polymers - Current and Future Ultrasound Applications*, B. R. McAvoy, Ed., IEEE, New York (1992), Vol. 1 & 2, p.539-550.
72. B. A. Newman, K. G. Kim, and J. I. Scheinbeim, *J. Mater. Sci.*, 25, 1779, (1990)
73. Q. X. Chen and P. A. Payne, *Meas. Sci. Technol.*, 6, 249, (1995)
74. D. K. Kharat, S. Mitra, S. Akhtar, and V. Kumar, *Def. Sci. J.*, 57, 7, (2007)
75. A. J. Holden, A. D. Parsons, and A. E. J. Wilson, *J. Acoust. Soc. Am.*, 73, 1858, (1983)
76. H. B. Miller, Patent No. 4376302, USPTO, (1983)
77. P. A. Lewin, *Ultrasonics*, 19, 213, (1981)
78. Y. Nakamura and T. Otani, *J. Acoust. Soc. Am.*, 94, 1191, (1993)
79. T. A. Henriquez and R. Y. Ting, *Jpn. J. Appl. Phys.*, 24S2, 876, (1985)
80. R. G. Swartz and J. D. Plummer, *IEEE Trans. Electron Devices*, 26, 1921, (1979)
81. B. Zhu and V. K. Varadan, in *Integrated MOSFET based hydrophone-device for underwater applications*, V. K. Varadan, Ed., Spie-Int Soc Optical Engineering, Bellingham (2002), Vol. 4700, p.101-110.

- 82.** P. Lum, M. Greenstein, C. Grossman, and T. L. Szabo, IEEE Trans. Ultrason. Ferroelectr. Freq. Control, 43, 536, **(1996)**
- 83.** M. S. Martins, V. Correia, S. Lanceros-Mendez, J. M. Cabral, and J. G. Rocha, in *Comparative finite element analyses of piezoelectric ceramics and polymers at high frequency for underwater wireless communications*, B. Jakoby and M. J. Vellekoop, Ed., Elsevier Science Bv, Amsterdam **(2010)**, Vol. 5, p.99-102.
- 84.** M. Tatoulian, F. Cavalli, G. Lorang, J. Amouroux, and F. Arefi-Khonsari, in *Polymer Surface Modification: Relevance to Adhesion*, K. L. Mittal, Ed., Brill, Leiden **(2009)**, Vol. 5, p.183-197.
- 85.** L. F. Brown, IEEE Transactions on Ultrasonics Ferroelectrics and Frequency Control, 47, 1377, **(2000)**
- 86.** R. E. Newnham, Ferroelectrics, 68, 1, **(1986)**
- 87.** A. Safari, J. Phys. III, 4, 1129, **(1994)**
- 88.** E. K. Akdogan, M. Allahverdi, and A. Safari, IEEE Transactions on Ultrasonics Ferroelectrics and Frequency Control, 52, 746, **(2005)**
- 89.** *Piezoelectric Brochure*, Morgan Electro Ceramics, **(2007)**
- 90.** *Properties of AIRMAR Piezoflex<sup>TM</sup> Piezoelectric Polymer*, AIRMAR Technology Corporation, **(1999)**, <http://www.airmartechonology.com/uploads/AirPDF/Piezoflex.pdf>
- 91.** S. Turcu, B. Jadidian, S. C. Danforth, and A. Safari, J. Electroceram., 9, 165, **(2002)**
- 92.** Q. C. Xu, S. Yoshikawa, J. R. Belsick, and R. E. Newnham, IEEE Trans. Ultrason. Ferroelectr. Freq. Control, 38, 634, **(1991)**
- 93.** A. E. Panich, V. Y. Topolov, S. V. Glushanin, and P. Kut, in *High-performance 1-3-type relaxor-ferroelectric-based composites*, Kaunas Univ Technology Press, Kaunas **(2006)**

- 94.** J. F. Tressler, A. Dogan, J. F. Fernandez, J. T. Fielding, Jr., K. Uchino, and R. E. Newnham, IEEE Ultrasonics Symposium Proceedings, 2, 897-900, **(1995)**
- 95.** W. Hackenberger, M. J. Pan, D. Kuban, T. Ritter, and T. Shrout, in *Novel method for producing high frequency 2-2 composites from PZT ceramic*, S. C. Schneider, M. Levy and B. R. McAvoy, Ed., **(2000)**, Vol. 1 & 2, p.969-972.
- 96.** K. Rittenmeyer, T. Shrout, W. A. Schulze, and R. E. Newnham, Ferroelectrics, 41, 323, **(1982)**
- 97.** C. Van Hoy, A. Barda, M. Griffith, and J. W. Halloran, J Am Ceram Soc, 81, 152, **(1998)**
- 98.** J. Cesarano, T. A. Baer, and P. Calvert, in *Recent developments in freeform fabrication of dense ceramics from slurry deposition*, D. L. Bourell, J. J. Beaman, R. H. Crawford, H. L. Marcus and J. W. Barlow, Ed., **(1997)**, Vol. p.25-32.
- 99.** K. Han, A. Safari, and R. E. Riman, J Am Ceram Soc, 74, 1699, **(1991)**
- 100.** H. Banno and S. Saito, Jpn. J. Appl.Phys., 22S2, 67, **(1983)**
- 101.** H. Banno, Ferroelectrics, 50, 329, **(1983)**
- 102.** H. Banno, K. Ogura, H. Sobue, and K. Ohya, Jpn. J. Appl.Phys., 26S1, 153, **(1987)**
- 103.** L. Li and N. R. Sottos, Ferroelectrics Lett., 21, 41, **(1996)**
- 104.** L. Li and N. R. Sottos, J. Appl. Phys., 77, 4595, **(1995)**
- 105.** S. Y. Lynn, *Polymer-piezoelectrics with 1-3 connectivity for hydrophone applicatons*, M.S. thesis, Pennsylvania State University, State College, PA, **(1981)**
- 106.** M. J. Haun, *Transverse reinforcement of 1-3 and 1-3-0 PZT polymer composites with glass fibers*, M.S. thesis, Pennsylvania State University, **(1983)**
- 107.** C. Richard, P. Eyraud, L. Eyraud, D. Audigier, and M. Richard, Proceedings of the Eighth IEEE International Symposium on Applications of Ferroelectrics, 255-258, **(1992)**

- 108.** J. F. Saillant, S. Cochran, R. Berriet, K. Kirk, and G. Fleury, Ultrasonics, 2003 IEEE Symposium on, 2, 2007-2010 Vol.2, **(2003)**
- 109.** J. F. Saillant, S. Cochran, R. Berriet, K. Kirk, and G. Fleury, Ultrasonics Symposium, 2004 IEEE, 1, 630-633 Vol.1, **(2004)**
- 110.** S. Yongan and X. Qiang, IEEE Trans. Ultrason. Ferroelectr. Freq. Control, 44, 1110, **(1997)**
- 111.** R. P. Schaeffer, V. F. Janas, and A. Safari, Proceedings of the Tenth IEEE International Symposium on Applications of Ferroelectrics, 2, 557-560 vol.2, **(1996)**
- 112.** K. S. Challagulla and T. A. Venkatesh, Philos. Mag., 89, 1197, **(2009)**
- 113.** R. E. Newnham, A. Dogan, Q. C. Xu, K. Onitsuka, J. Tressler, and S. Yoshikawa, IEEE Ultrasonics Symposium Proceedings, 509-513 vol.1, **(1993)**
- 114.** P. Ochoa, J. L. Pons, M. Villegas, and J. F. Fernandez, Sens. Actuators, A, 132, 63, **(2006)**
- 115.** R. J. Meyer, W. J. Hughes, T. C. Montgomery, D. C. Markley, and R. E. Newnham, J. Electroceram., 8, 163, **(2002)**
- 116.** P. Ochoa, M. Villegas, J. L. Pons, P. Leidinger, and J. F. Fernández, J. Electroceram., 14, 221, **(2005)**
- 117.** R. E. Newnham, J. Zhang, and R. Meyer, Jr., Proceedings of the 2000 12th IEEE International Symposium on Applications of Ferroelectrics, 1, 29-32 vol. 1, **(2000)**
- 118.** J. D. Zhang, W. J. Hughes, A. C. Hladky-Hennion, and R. E. Newnham, Materials Research Innovations, 2, 252, **(1999)**
- 119.** P. Marin-Franch, S. Cochran, and K. Kirk, J. Mater. Sci. - Mater. Electron., 15, 715, **(2005)**
- 120.** Z. Xu, F. T. Chen, Z. Z. Xi, Z. R. Li, L. H. Cao, Y. J. Feng, and X. Yao, Ceram. Int., 30, 1777, **(2004)**



- 121.** T. Ritter, G. Xuecang, K. Kirk Shung, P. D. Lopath, P. Seung-Eek, and T. R. Shrout, IEEE Trans. Ultrason. Ferroelectr. Freq. Control, 47, 792, **(2000)**
- 122.** J. Zhao, Q. M. Zhang, N. Kim, and T. Shrout, Jpn. J. Appl.Phys., 34, 5658, **(1995)**
- 123.** J. Kuwata, K. Uchino, and S. Nomura, Ferroelectrics, 37, 579, **(1981)**
- 124.** S. E. Park and T. R. Shrout, J. Appl. Phys., 82, 1804, **(1997)**
- 125.** K. Tashiro, H. Tadokoro, and M. Kobayashi, Ferroelectrics, 32, 167, **(1981)**
- 126.** *Electro-Ceramic Products and Material Specification*, ITT Corporation, **(2010)**
- 127.** *EBL Lead Zirconate Titanate Characteristics*, EBL Products Inc., **(2012)**,  
<http://www.eblproducts.com/leadzirc.html>
- 128.** G. H. Haertling, J Am Ceram Soc, 82, 797, **(1999)**
- 129.** Y. Ye, H. Huang, L. Zhou, S. Wang, and S. Yu, J Am Ceram Soc, 93, 2244, **(2010)**
- 130.** *Single Crystal Materials*, TRS Technologies, Inc., **(2010)**,  
[http://www.trstechnologies.com/Materials/single\\_crystals.php](http://www.trstechnologies.com/Materials/single_crystals.php)
- 131.** *Specifications of PMN-PT Single Crystal (PMN-32%PT)*, APC International, Ltd., **(2011)**,  
<http://www.americanpiezo.com/product-service/pmn-pt.html>
- 132.** J. S. Harrison and Z. Ounaies, *Piezoelectric Polymers*, ICASE, NASA Langley Research Center, Report No. 2001-43 **(2001)**
- 133.** S. C. Butler, J. L. Butler, A. L. Butler, and G. H. Cavanagh, J. Acoust. Soc. Am., 102, 308, **(1997)**
- 134.** L. E. Cross, *Materials for Adaptive Structural Acoustic Control* Office of Naval Research, Report No. N00014-92-J-1510 **(1993)**

**List of tables:**

Table 1: Typical properties of various types of piezoelectric ceramics.

Table 2: Typical properties of relaxor ferroelectric single crystals compared to Navy Type 6 PZT ceramics.

Table 3: Typical properties of PVDF and its copolymers.

## List of figures:

Fig. 1. Schematic of the perovskite structure ( $ABO_3$ ) with  $BaTiO_3$  as an example.

Fig. 2. Phase diagram of the  $PbZrO_3$ - $PbTiO_3$  solid solution [17].

Fig. 3. Variation of the room-temperature piezoelectric properties of  $PbZrO_3$ - $PbTiO_3$  with composition [17].

Fig. 4. Source levels of a hollow cylindrical PZT transducer made from different types of PZT ceramics when driven at the same voltage.

Fig. 5. Phase diagrams of PMN-PT (a) and PZN-PT (b) solid solutions. Reprinted with permission from [122], J. Zhao et al., *Jpn. J. Appl. Phys.* 34, 5658 (1995) © 1995 Publication Board, Japanese Journal of Applied Physics, and [123], J. Kuwata et al., “Phase-transitions in the  $Pb(Zn_{1/3}Nb_{2/3})O_3$ - $PbTiO_3$  System,” *Ferroelectrics* 37, 579 (1981) © 1981 Taylor & Francis Ltd, <http://www.tandf.co.uk./journals>.

Fig. 6. Dielectric constant and polarization behavior of PMN as a function of temperature. Reprinted with permission from [8], T. R. Shrout et al., *IEEE 1990 Ultrasonics Symposium : Proceedings, 1-3*, 711 (1990) © 1990 IEEE.

Fig. 7. Illustration of E-field-induced ferroelectric rhombohedral-tetragonal phase transition of  $\langle 001 \rangle$  oriented rhombohedral PZN-PT single crystals under DC bias. Reprinted with permission from [124] S. E. Park et al. *J. Appl. Phys.* 82, 1804 (1997) © 1997, American Institute of Physics.

Fig. 8. Crystalline structures of PVDF. Reprinted with permission from [125], K. Tashiro et al., “Structure and piezoelectricity of poly(vinylidene fluoride),” *Ferroelectrics* 32, 167 (1981) © 1981 Taylor & Francis Ltd, <http://www.tandf.co.uk./journals>.

Fig. 9. Comparison of FOM ( $d_{hg_h}$ ) of different piezoelectric materials reported in the literature.

Fig. 10. Three typical connectivity patterns of diphasic piezoelectric composites used in underwater acoustic transducers.

Table 1: Typical properties of various types of piezoelectric ceramics.

	Symbol	Unit	Navy	Navy	Navy	Navy	Navy	PMN-	PNN-
			Type 1	Type 2	Type 3	Type 5	Type 6	35%PT	36%PT
Material product name			EC-64	PZT5A2	EC-69	EBL#6	PZT5H2		
Dielectric constant (at 1 kHz)	$K_{33}^T$		1300	1700	1050	2750	3400	3640	6170
Dielectric loss (at 1 kHz)	$\tan\delta$		0.004	0.02	0.003	0.020	0.025		
Mechanical Quality Factor	$Q_m$		400	75	900	75	65		
Piezoelectric charge coefficient	$d_{33}$	$10^{-12}\text{C/N}$	295	374	220	480	593	563	570
	$d_{31}$	$10^{-12}\text{C/N}$	-127	-171	-95	-260	-274	-241	
Electromechanical coupling coefficient	$k_p$		0.60	0.60	0.52	0.63	0.65	0.58	
	$k_{33}$		0.71	0.71	0.62	0.74	0.75	0.70	
Young's modulus	$Y_{33}^E$	GPa	67	53	74		48		
Curie point	$T_c$ or $T_m$	$^{\circ}\text{C}$	320	374	300	220	200	185	88
Reference			[126]	[89]	[126]	[127]	[89]	[128]	[129]

Table 2: Typical properties of relaxor ferroelectric single crystals compared to Navy Type 6 PZT ceramics.

	Crystal orientation	Dielectric constant	$d_{33}$ (pC/N)	$k_{33}$	Ref.
PMN-32%PT	<001>	8000	1800-2000	0.91	[130]
	<111>	3500	450		[131]
PZN-8%PT	<001>	5000	2500	0.94	[124]
	<111>	1000	84	0.39	
Navy Type 6 PZT		3400	593	0.75	[89]

Table 3: Typical properties of PVDF and its copolymers.

	PVDF	P(VDF-TrFE)	P(VDF-TeFE)	P(VDC N-VAc)	Ref.
Dielectric constant $\epsilon_r$	6.0	5.0	5.5	6.0	[71]
Dielectric loss factor $\tan\delta$	0.25	0.12	0.20		[71]
Mechanical quality factor $Q_m$	10	25	15		[71]
Piezoelectric charge constant $d_{33}$ (pC/N)	25	12.5			[73]
Piezoelectric charge constant $d_{31}$ (pC/N)	12-23	9-12.5		6-10	[70, 132]
Hydrostatic piezoelectric voltage constant $g_h$ ( $10^{-3}\text{Vm/N}$ )	90	170-275			[133, 134]
Electro-mechanical coupling factor $k_r$	0.20	0.30	0.21	0.22	[71]
Acoustic impedance $Z$ (MRayls)	3.9	4.5	4.2	3.1	[71]

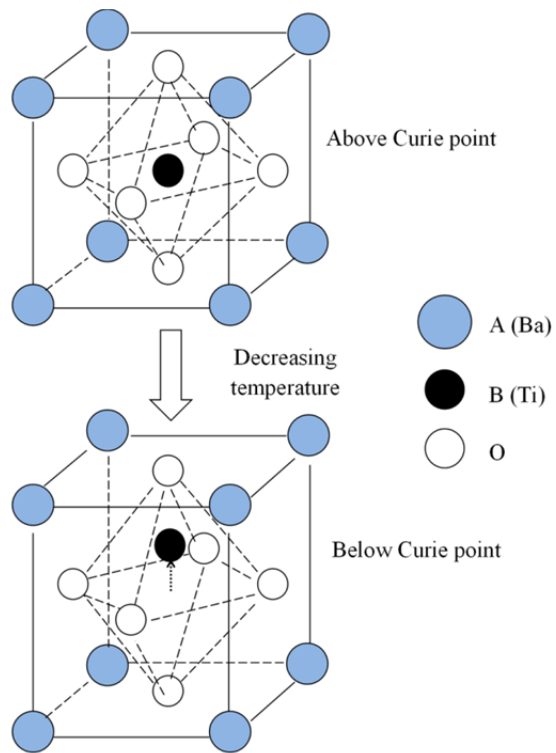


Fig. 1. Schematic of the perovskite structure (ABO<sub>3</sub>) with BaTiO<sub>3</sub> as an example.

**Manuscript title:** *Piezoelectric Materials Used in Underwater Acoustic Transducers*

**Authors:** Huidong Li, Z. Daniel Deng and Thomas J. Carlson



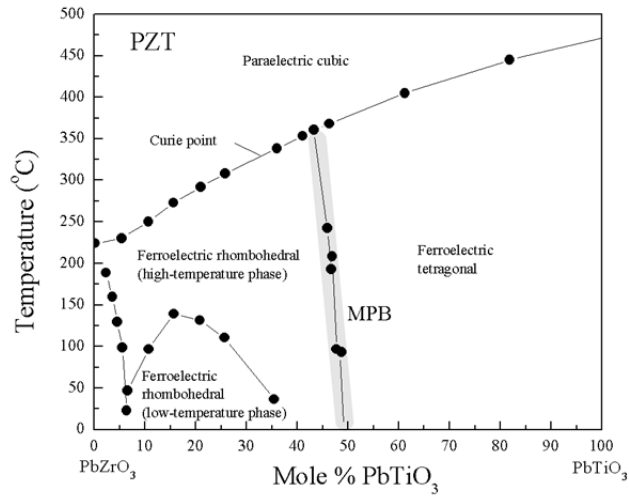


Fig. 2. Phase diagram of the  $\text{PbZrO}_3$ - $\text{PbTiO}_3$  solid solution [17].

**Manuscript title:** *Piezoelectric Materials Used in Underwater Acoustic Transducers*  
**Authors:** Huidong Li, Z. Daniel Deng and Thomas J. Carlson

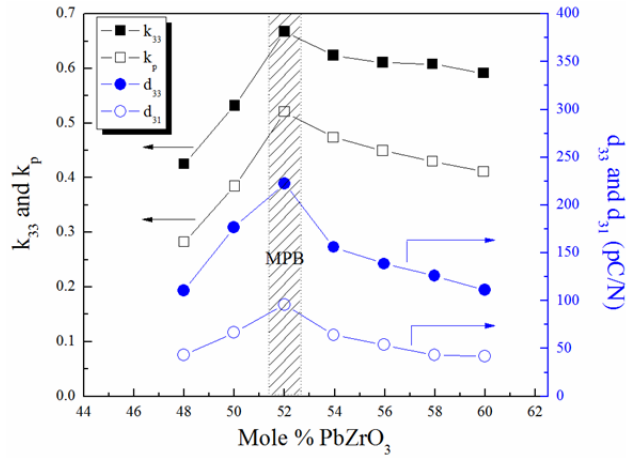


Fig. 3. Variation of the room-temperature piezoelectric properties of PbZrO<sub>3</sub>-PbTiO<sub>3</sub> with composition [17].

**Manuscript title:** *Piezoelectric Materials Used in Underwater Acoustic Transducers*  
**Authors:** Huidong Li, Z. Daniel Deng and Thomas J. Carlson

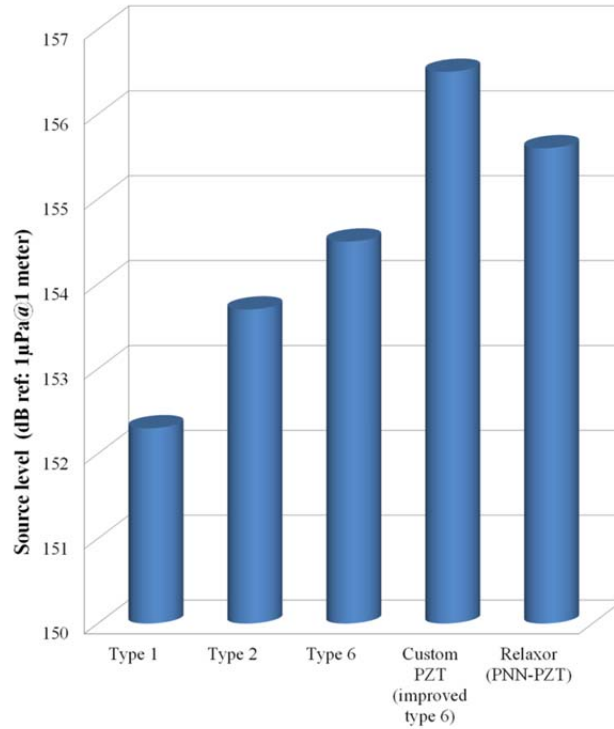


Fig. 4. Source levels of a hollow cylindrical PZT transducer made from different types of PZT ceramics when driven at the same voltage.

**Manuscript title:** *Piezoelectric Materials Used in Underwater Acoustic Transducers*  
**Authors:** Huidong Li, Z. Daniel Deng and Thomas J. Carlson

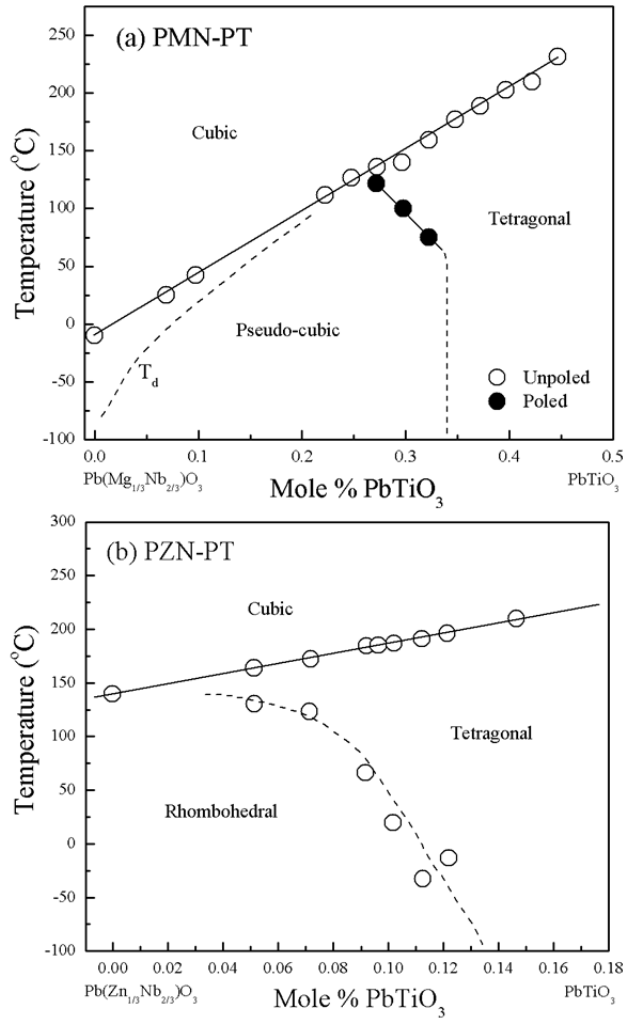


Fig. 5. Phase diagrams of PMN-PT (a) and PZN-PT (b) solid solutions. Reprinted with permission from [122], J. Zhao et al., *Jpn. J. Appl. Phys.* 34, 5658 (1995) © 1995 Publication Board, Japanese Journal of Applied Physics, and [123], J. Kuwata et al., “Phase-transitions in the Pb(Zn<sub>1/3</sub>Nb<sub>2/3</sub>)O<sub>3</sub>-PbTiO<sub>3</sub> System,” *Ferroelectrics* 37, 579 (1981) © 1981 Taylor & Francis Ltd, <http://www.tandf.co.uk/journals>.

**Manuscript title:** *Piezoelectric Materials Used in Underwater Acoustic Transducers*  
**Authors:** Huidong Li, Z. Daniel Deng and Thomas J. Carlson

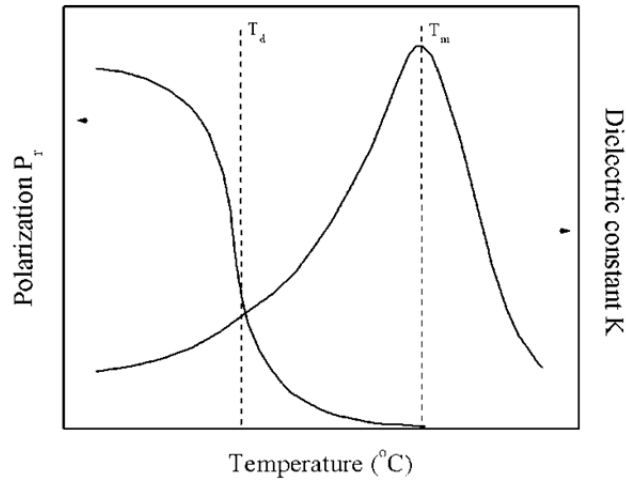


Fig. 6. Dielectric constant and polarization behavior of PMN as a function of temperature.

Reprinted with permission from [8], T. R. Shrout et al., *IEEE 1990 Ultrasonics Symposium : Proceedings*, 1-3, 711 (1990) © 1990 IEEE.

**Manuscript title:** *Piezoelectric Materials Used in Underwater Acoustic Transducers*  
**Authors:** Huidong Li, Z. Daniel Deng and Thomas J. Carlson

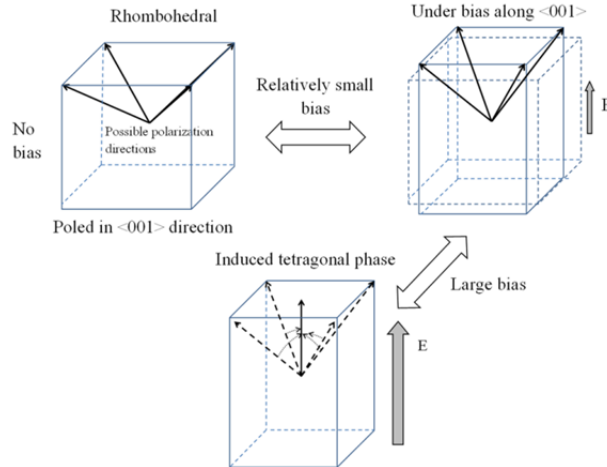


Fig. 7. Illustration of E-field-induced ferroelectric rhombohedral-tetragonal phase transition of  $\langle 001 \rangle$  oriented rhombohedral PZN-PT single crystals under DC bias. Reprinted with permission from [124], S. E. Park et al. *J. Appl. Phys.* 82, 1804 (1997) © 1997, American Institute of Physics.

**Manuscript title:** *Piezoelectric Materials Used in Underwater Acoustic Transducers*  
**Authors:** Huidong Li, Z. Daniel Deng and Thomas J. Carlson

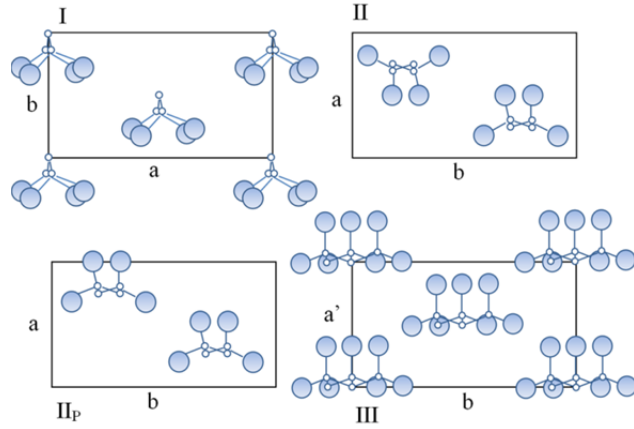


Fig. 8. Crystalline structures of PVDF. Reprinted with permission from [125], K. Tashiro et al., “Structure and piezoelectricity of poly(vinylidene fluoride),” *Ferroelectrics* 32, 167 (1981) © 1981 Taylor & Francis Ltd, <http://www.tandf.co.uk./journals>.

**Manuscript title:** *Piezoelectric Materials Used in Underwater Acoustic Transducers*  
**Authors:** Huidong Li, Z. Daniel Deng and Thomas J. Carlson

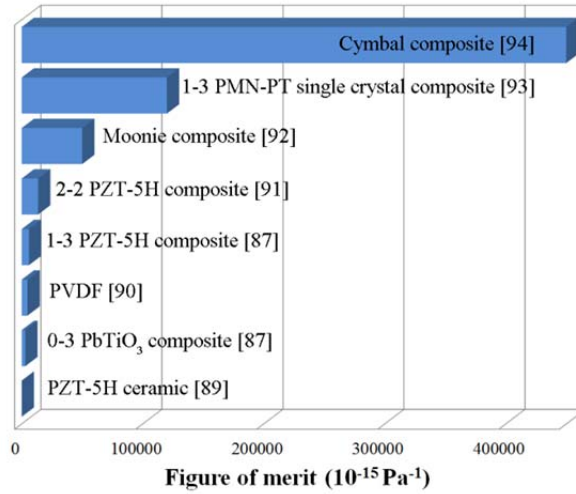


Fig. 9. Comparison of FOM ( $d_{hg}$ ) of different piezoelectric materials reported in the literature.

**Manuscript title:** *Piezoelectric Materials Used in Underwater Acoustic Transducers*  
**Authors:** Huidong Li, Z. Daniel Deng and Thomas J. Carlson



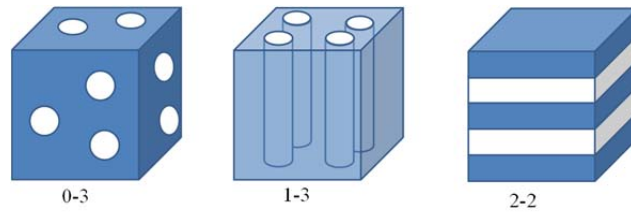


Fig. 10. Three typical connectivity patterns of diphasic piezoelectric composites used in underwater acoustic transducers.

**Manuscript title:** *Piezoelectric Materials Used in Underwater Acoustic Transducers*  
**Authors:** Huidong Li, Z. Daniel Deng and Thomas J. Carlson